

Investigation of Nitrile Oxide-Alkyne 1,3-Dipolar Cycloadditions and Their Potential  
Viability for Synthesis of Stapled Peptides

by

Charles Teeple

A thesis presented to the Honors College of Middle Tennessee State University in partial  
fulfillment of the requirements for graduation from the University Honors College.

Fall 2020

Investigation of Nitrile Oxide-Alkyne Cycloadditions and Their Potential Viability for Synthesis  
of Stapled Peptides

by Charles Teeple

APPROVED:

---

Dr. Norma Dunlap, Thesis Director  
Professor, Department of Chemistry

---

Dr. Scott Handy, Second Reader  
Professor, Department of Chemistry

---

Dr. Gregory Van Patten, Thesis Committee Chair  
Chair, Department of Chemistry

## **Acknowledgments**

This project would not be possible without my advisor, Dr. Norma Dunlap. I appreciate all the time she spent teaching me the basics of organic synthesis in the lab, as well as the writing advice she gave me outside the lab. I also want to thank my mom and grandmother (Jane and Jewell) who supported me and encouraged my academic pursuits. Finally, I want to thank my girlfriend, Ida, who gave me support during the long days and nights needed to finish this project.

## Abstract

The nitrile oxide-alkyne 1,3-dipolar cycloaddition reaction is a concerted reaction between a nitrile oxide, which is usually generated *in situ*, and an alkyne to afford an isoxazole. This reaction has been previously used in post-synthetic modification of nucleic acids. This work examines the potential utility of the nitrile oxide-alkyne 1,3-dipolar cycloaddition reaction in the synthesis of stapled peptides. Stapled peptides, or hydrocarbon cross-linked peptides, show potential as drugs to target protein-protein interactions in the body. The nitrile oxide-alkyne cycloaddition, if efficient, could solve some of the issues currently present in stapled peptide synthesis, including the use of toxic copper catalysts in the more common azide-alkyne 1,3-dipolar cycloaddition. Multiple nitrile oxide-alkyne cyclization attempts proved successful with simple starting materials. Subsequently, two amino acids, one containing an aldehyde and another containing an alkyne, were synthesized. The amino acids were not able to successfully participate in the nitrile oxide-alkyne cycloaddition. More research is required to optimize the procedure for this reaction before it can be used in a stapled peptide.

## Table of Contents

<b>List of Figures</b>	<b>v</b>
<b>List of Tables</b>	<b>vi</b>
<b>Chapter I: Introduction</b>	<b>1</b>
<b>Background</b>	<b>1</b>
<b>Targeting Protein-Protein Interactions</b>	<b>3</b>
<b>Stapled Peptides</b>	<b>5</b>
<b>Chapter II: Materials and Methods</b>	<b>14</b>
<b>General Experimental Details</b>	<b>14</b>
<b>Synthesis of Isoxazoles from 1-Hexyne and Simple Aldehydes</b>	<b>15</b>
<b>Synthesis of Alkyne and Aldehyde Amino Acids</b>	<b>19</b>
<b>Chapter III: Results and Discussion</b>	<b>23</b>
<b>Conclusion</b>	<b>31</b>
<b>References</b>	<b>32</b>
<b>Appendix</b>	<b>35</b>

## List of Figures

<b>Figure 1. Acetylcholinesterase interacting with a small molecule.</b>	<b>2</b>
<b>Figure 2. Examples of peptide-like molecules designed to target PPI.</b>	<b>4</b>
<b>Figure 3. Representation of an <math>\alpha</math>-helix.</b>	<b>5</b>
<b>Figure 4. Examples of different types of stapled peptides.</b>	<b>6</b>
<b>Figure 5. Example of RCM in solid phase stapled peptide synthesis.</b>	<b>8</b>
<b>Figure 6. Examples of the 1,3-dipolar cycloaddition.</b>	<b>10</b>
<b>Figure 7. Nitrile oxide and alkyne 1,3-dipolar cycloaddition.</b>	<b>11</b>
<b>Figure 8. Examples of the NOAC reaction being used with DNA.</b>	<b>12</b>
<b>Figure 9. Schematic of the final stapled peptide created with the NOAC reaction.</b>	<b>13</b>
<b>Scheme 1. (a) Schematic for synthesis of 5-butyl-3-phenylisoxazole (4) and 4-butyl-3-phenylisoxazole from benzaldehyde.</b>	<b>15</b>
<b>Scheme 2. Schematic for synthesis of homopropargyl glycine.</b>	<b>19</b>
<b>Scheme 3. Schematic for synthesis of aspartic acid <math>\beta</math>-semialdehyde.</b>	<b>22</b>
<b>Figure 10. Mechanism and examples of nitrile oxide dimerization to furoxans</b>	<b>24</b>
<b>Figure 11. Proposed mechanism of acid catalyzed hydrolysis of the expected nitrile product.</b>	<b>27</b>
<b>Scheme 4. Reduction attempts the achieve the desired aldehyde.</b>	<b>28</b>
<b>Scheme 5. Attempted oxidation reactions with amino acid alcohols.</b>	<b>29</b>
<b>Scheme 6. Successful synthesis of Fmoc-<i>L</i>-aspartic acid <math>\beta</math>-semialdehyde.</b>	<b>30</b>
<b>Scheme 7. Failed cyclization attempts with unnatural amino acids.</b>	<b>31</b>

## List of Tables

<b>Table 1. Conditions, hydroximidoyl chloride age, and percent yields for cyclization attempts with 1-hexyne.</b>	<b>26</b>
--	-----------

## CHAPTER I: INTRODUCTION

### Background

Pharmaceutical drugs are molecules that are used to treat disease (1). Throughout most of history, drugs were natural compounds that were extracted from plants, many being amine-containing alkaloids. Now, most approved drugs are created in a lab by medicinal chemists using synthetic organic chemistry. Current knowledge of organic synthesis allows medicinal chemists to fine tune the structures of known molecules or create new ones altogether, leading to a wide range of structural possibilities. Molecules that show promise as drugs must then be rigorously tested for safety and efficacy to be approved for human use. For a drug to produce its desired effect, it must interact with a specific biological structure known as the target (1, 2, 3). The way a drug interacts with a specific target to produce a biological effect is known as its mechanism of action, and knowledge of this is generally necessary for a drug to be approved (1). This entire process of a drug interacting with its target is driven by thermodynamics (3). To further understand drug design, it is necessary to distinguish between “macromolecules” and “small molecules.”

Macromolecules are molecules that are large and complex. Common examples of macromolecules are biological polymers like proteins, DNA, and polysaccharides (1). Proteins interact with other proteins and biomolecules to perform a variety of vital functions, including mediation of metabolism, biosignaling, and other cellular processes. However, endogenous proteins with abnormal structure or expression levels can cause

disease, which makes proteins in biochemical pathways common drug targets (1, 4).

Other common macromolecular targets include RNA and DNA (1).

“Small molecules” are molecules or ligands that are small in relation to macromolecules and generally accessible via organic synthesis. Most approved drugs are small molecules that have a macromolecular target. The most common macromolecular targets for small molecules are enzymes and receptors, which are both proteins. The small molecule drug interacts with these structures by fitting into a defined binding pocket. The interaction of the drug with the binding site causes a change in the protein’s activity within the body. The presence of a binding site allows a small molecule drug to be designed to tightly interact with its target (1, 2, 3). An example of a small molecule interacting with a macromolecule is shown below in **Figure 1**, which shows the enzyme acetylcholinesterase interacting with the small molecule C7653.

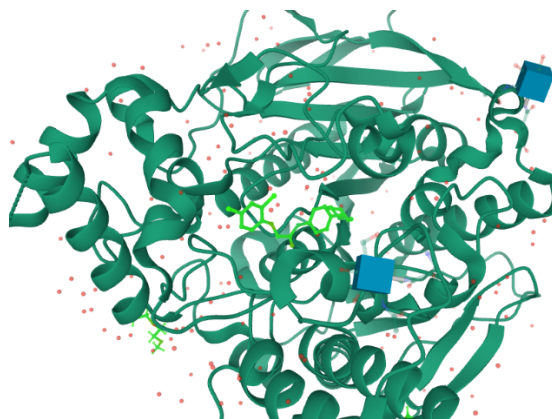


**Figure 1.** Acetylcholinesterase interacting with a small molecule. The macromolecule in dark green is acetylcholinesterase. The lime green structure represents a small molecule that is interacting with its binding site. This small molecule is a research chemical known as C7653 (5).

Drugs can also be macromolecules. Macromolecular drugs are known as “biologics” and they are generally isolated or engineered from living organisms. Examples include vaccines, gene therapies, and antibody-drug conjugates. Being large, complex structures, biologics have very specific applications and can interact with biochemical pathways that are inaccessible to small molecule drugs (1, 6). However, due to their complexity, the structures of biologics are not easily characterized. Other issues with biologics include poor cell penetration and the fact that oral administration is infeasible (6, 7). On the other hand, small molecule drugs can be administered orally and easily penetrate cells but lack the size or structural complexity to interact with targets that do not have a defined binding site (7, 8).

### **Targeting Protein-Protein Interactions**

Some interactions or potential targets are still inaccessible by conventional small molecule drugs and biologics. Some of these interactions include intracellular protein-protein interactions (PPI). Like the name implies, protein-protein interactions are between two macromolecules. These interactions are numerous within cells and are predominate in a variety of important biochemical pathways. Small molecules are generally of limited use to target these interactions because there are usually no defined binding pockets on the macromolecules in question. Instead, there are usually flat surfaces around 15 Å in size that can participate in multiple weak interactions. In the absence of a binding pocket, small molecule drugs can sometimes be designed to bind to “hot spots,” which are residues on the surface that play a large role in protein binding, but this strategy is not always effective. Biologics could potentially be a promising solution to this issue, but biologics have poor cell penetration and therefore cannot get to the areas where these

interactions occur. These issues have been solved by creating new classes of drugs that specifically target PPI and have some characteristics of both biologics and small molecules (7, 8, 9).

Some drugs targeting PPI are modified peptides, or short amino acid sequences, that mimic a vital piece of one of the macromolecules involved in the PPI. Peptide-like drugs are small enough to penetrate cells, yet complex enough to bind to proteins that are part of a PPI. The modifications of the peptides are crucial to their potential as effective drugs. Unmodified peptides are quickly metabolized inside the body before they have a chance to penetrate cells. Also, the peptide must adopt a specific three-dimensional conformation to bind to the target protein, and free peptides generally do not adopt this active conformation readily. Modification solves both issues (7, 8, 9, 10). Examples of some types of drugs that target PPI are shown below in **Figure 2** compared to an unmodified peptide. Peptoids are peptides with amino acid R-groups shifted from the alpha carbon to the nitrogen (8, 11). Stapled peptides are normal peptides with a hydrocarbon or heterocyclic cross link, or “staple,” that induces stability of the three-dimensional structure (7, 8, 9, 10).

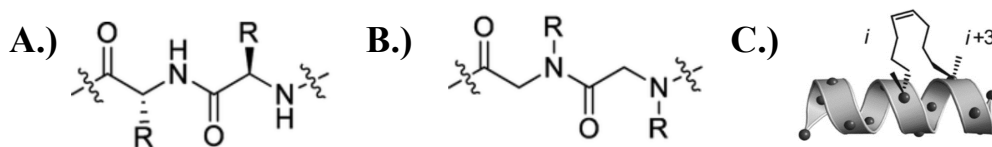


**Figure 2.** Examples of peptide-like molecules designed to target PPI. **A.)** represents an unmodified peptide with its R-groups attached to the  $\alpha$ -carbon (10). **B.)** represents the basic structure of peptoids, which differ from peptides in that the R-groups are attached to the nitrogen of the amide bond (10). **C.)** is a representation of an  $\alpha$ -helical stapled peptide with a hydrocarbon cross-link (7).

## Stapled Peptides

$\alpha$ -Helical stapled peptides will be the focus of this work, and they will now be explored in more depth. First, it is important to understand the conformational component. For macromolecules (proteins) in a normal PPI to interact, they must be folded into the correct active conformation. One structure common in PPI motifs is the  $\alpha$ -helix (7, 9, 10). Some characteristics of the  $\alpha$ -helix are shown in **Figure 3**.

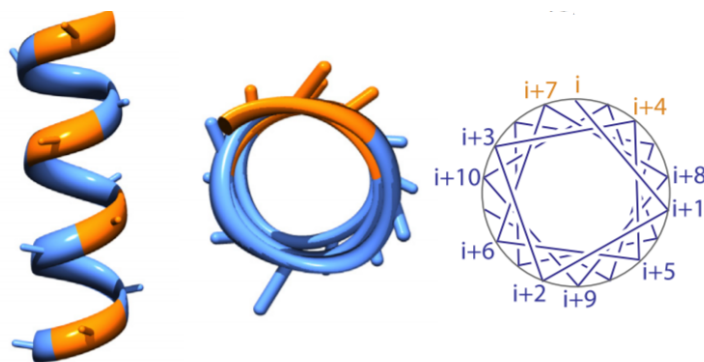


**Figure 3.** Representation of an  $\alpha$ -helix. A side view of the helix is on the left and a top view is in the center (each spike is an amino acid chain). The rightmost drawing shows the locations of individual amino acid residues  $i - i+10$  in the helix. One turn of the  $\alpha$ -helix includes 3.6 amino acid residues (12).

Stapled peptides must also adopt this  $\alpha$ -helical conformation to effectively bind to the target. The synthetic “staple” is covalently attached at two points to amino acid residues of the peptide and restricts the number of possible conformations that the peptide can sample in solution. This restriction of movement makes the  $\alpha$ -helical conformation of the stapled peptide much more stable, and therefore more likely to persist, compared to the unmodified version of the peptide. This is analogous to stapling a stack of papers to keep them together in the correct order. To properly stabilize the  $\alpha$ -helix, the staple must

attach at very specific amino acids on the peptide and be of the correct length. As noted in **Figure 3**, 3.6 amino acids comprise a single  $\alpha$ -helical turn. Therefore, most stapled peptides have two attachments at three or four amino acids apart, so the attachments are on the same side of the helix. Some staples span two  $\alpha$ -helical turns, or seven amino acids. Stapled peptides are generally named in terms of  $i$ , a variable that represents the amino acid residue where the first attachment of the staple is located, and  $i + x$ , which represents the amino acid residue where the other end of the staple attaches. For example, a stapled peptide with a staple that spans three amino acid residues, or about one turn, would be named as an “ $i, i + 3$  stapled peptide.” A stapled peptide that spans two  $\alpha$ -helical turns would be denoted as  $i, i + 7$ . The most common stapled peptides have staples that either span one or two turns.  $i, i + 3$  or  $i, i + 4$  for one turn, and  $i, i + 7$  for two turns. This spacing allows the ends of the staple to attach on the same side of the helix, which is crucial for helix stabilization (7, 9, 10). Examples are shown in **Figure 4**.

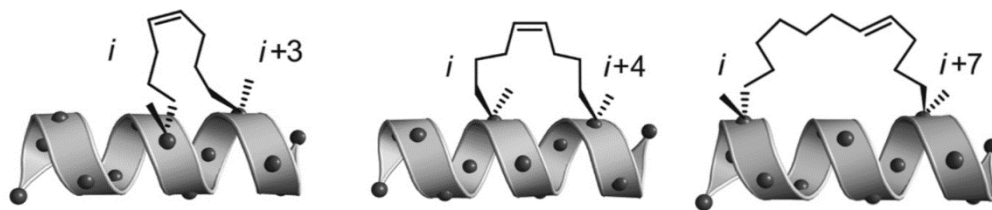


**Figure 4.** Examples of different types of stapled peptides. Three possibilities are:  $i, i+3$ ;  $i, i+4$ ; and  $i, i+7$  (7).

The location of the staple must be chosen carefully. The parts of the peptide that bind to the target are the R-groups, or variable groups, of the individual amino acid residues. For the two amino acid residues where the staple attaches, their natural R group is replaced with the staple itself. Therefore, for cross-link attachment points, it is

important to select amino acid residues that do not play a large role in the binding of the peptide to its target. This generally means picking amino acid residues that are not on the same side of the helix which interacts with the target. In some cases, the staple itself can also participate in binding as a hydrophobic moiety. For these reasons, structural information about the proteins in the target PPI is crucial. Some basic structural knowledge is also required to confirm that the peptide being synthesized has a natural propensity to form the  $\alpha$ -helix. If the peptide is unlikely to form an  $\alpha$ -helix in the first place, then the reactive ends of the alkyl chains are less likely to come into contact and react to stabilize the structure (7, 9, 10).

The other major function of the cross-link staple is to prevent metabolism *in vivo*. Free proteins or peptides are broken down by proteases, which are enzymes that break peptide bonds. The cross-link mitigates this for a few reasons. First, the  $\alpha$ -helical secondary structure that the cross-link stabilizes makes the peptide bond less accessible to proteases. In the alpha helical conformation, the R groups of the amino acid residues point outwards, making it more difficult for the catalytic site of a protease to access the peptide bond. Also, the staple itself can act as a physical barrier that keeps the enzyme from binding to the peptide and cleaving the amide bonds. The combined effect of the alpha helix and the staple allow the stapled peptide to exist long enough *in vivo* to interact with its target (7, 9, 10).

Stapled peptides are accessible through a combination of traditional organic synthesis techniques and solid phase peptide synthesis. A general method for stapled peptide synthesis will now be described. First, two unnatural amino acids that contain an alkyl chain with a terminal reactive moiety are created with liquid phase organic

synthesis. The alkyl chain with the reactive group replaces where an R group would be on a standard amino acid. Then, a peptide that incorporates the unnatural amino acids at the correct residues is created using solid phase peptide synthesis. Finally, the peptide is exposed to reagents that result in the coupling of the two reactive R groups present on the unnatural amino acids. The natural formation of an alpha helix by the peptide allows the R groups to react, and the subsequent coupling of those two groups results in the staple or cross-link, which stabilizes the  $\alpha$ -helix (7, 9, 10). The most used reactions for joining the two alkyl chains in the final step include olefin ring-closing metathesis and 1,3-dipolar cycloadditions (10).

Ring-closing metathesis (RCM) is the coupling of two terminal alkenes to form one cyclic alkene and a smaller alkene byproduct. The reagent used in this reaction is a ruthenium complex known as Grubbs' Catalyst. An example of RCM being used in stapled peptide synthesis is shown below in **Figure 5**.

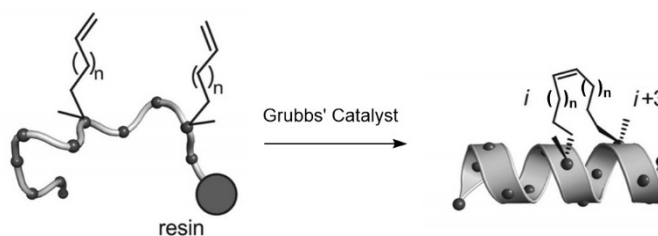


**Figure 5.** Example of RCM in solid phase stapled peptide synthesis. The two alkenes on the left react to form a macrocycle in the compound on the right (7).

Olefin RCM was the first reaction used to create stapled peptides. Blackwell and Grubbs originally used RCM to couple the side chains of two O-allyl homoserine amino acids (13). Inspired by this research, Verdine and co-workers introduced the concept of

peptide stapling by creating an all-hydrocarbon, side-chain to side-chain cross link in a peptide using RCM with the goal of structural stabilization (14). Later, the same research group reported an alpha helical stapled peptide derived from BH3 domain of the BCL-2 protein. The interaction it inhibited was the interaction of BCL-2 with pro-apoptotic proteins, which promote cell death. This stapled peptide was designed to target an intracellular PPI and showed *in vivo* antitumor activity, making it the first of its kind (15). This established olefin RCM as an effective reaction for future stapled peptide synthesis.

The other major reaction used for the staple formation is the 1,3-dipolar cycloaddition. Discovery and characterization of this reaction was done by Rolf Huisgen in the 1960s (16, 17, 18). The concerted reaction is between a dipole, which contains both a positive and negative charge, and a dipolarophile, which is usually an electron rich group like an alkene or alkyne. The resulting product is a 5-membered ring. Examples of stapled peptides that are made using the 1,3-dipolar cycloaddition generally utilize an azide group as the dipole and an alkyne as the dipolarophile, with the product being a triazole (16, 17, 18). The result of this is shown in **Figure 6**. The Cu(I) ion is generally used as a catalyst for this reaction due to the reaction's poor kinetics. Triazole stapled peptides as well as the mechanism for the reaction are shown below. This cycloaddition is a staple among a category of chemical reactions known as “click” reactions. This is an informal term used to describe reactions where two functional groups snap together as if they are parts of a buckle. Click reactions generally proceed under mild, benign solvent or solvent-free conditions and use readily accessible materials. Other characteristics include high predictability, spontaneity, and efficiency. These properties make click chemistry useful in biotechnology, drug design, and materials science (16, 17, 18).

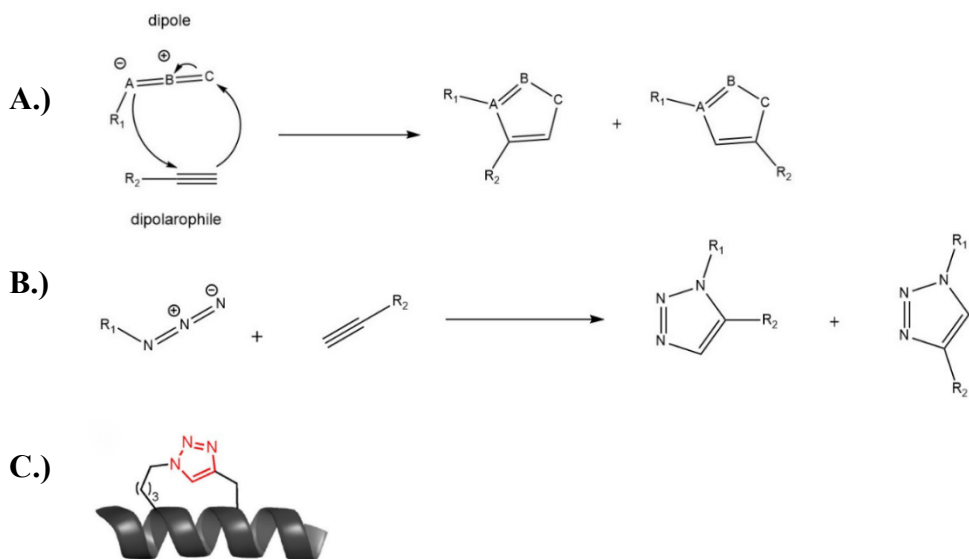


**Figure 6.** Examples of the 1,3-dipolar cycloaddition. **A.)** One-step mechanism of the 1,3-dipolar cycloaddition between a dipole and a dipolarophile. **B.)** Schematic of the basic reaction between an azide and an alkyne via 1,3-dipolar cycloaddition. **C.)** Example of a stapled peptide created via the azide-alkyne cycloaddition.

Though the copper (I) catalyzed azide-alkyne cycloaddition is the gold standard for click reactions and sees wide usage in a variety of fields, it is not without issues. Using starting materials capable of chelating copper ions can slow reaction progress. Furthermore, the requirement of a copper catalyst means that residual copper can be present in the product, requiring careful purification. Copper is cytotoxic, causing oxidative damage such as DNA degradation and protein denaturation. Residual copper from its use as a catalyst presents a challenge in the pharmaceutical industry, where the concentration of copper cannot exceed 15 ppm. Techniques like extensive washing, simple filtration, and nanoparticle exposure can mitigate residual copper amounts (16, 18).

Another useful 1,3-dipolar cycloaddition click reaction is the coupling of nitrile oxides and alkynes to afford isoxazoles, shown in **Figure 7**. Though the mechanism of this reaction is the same as the copper (I) catalyzed azide-alkyne reaction, the nitrile oxide cycloaddition behaves differently and may solve some of the problems associated with the use of azides. Kinetically, a nitrile oxide-alkyne cycloaddition (NOAC) is much faster than the uncatalyzed azide version, and therefore a metal catalyst is generally optional. Furthermore, nitrile oxide dipoles, though more reactive, are safer to handle than azides. However, due to their reactivity, they are prone to dimerization, where they react with each other rather than the dipolarophile (16, 18, 19). This can be mitigated with *in situ* generation of the nitrile oxide from an oxime, which is shown in Figure 7 along with the mechanism for the reaction.

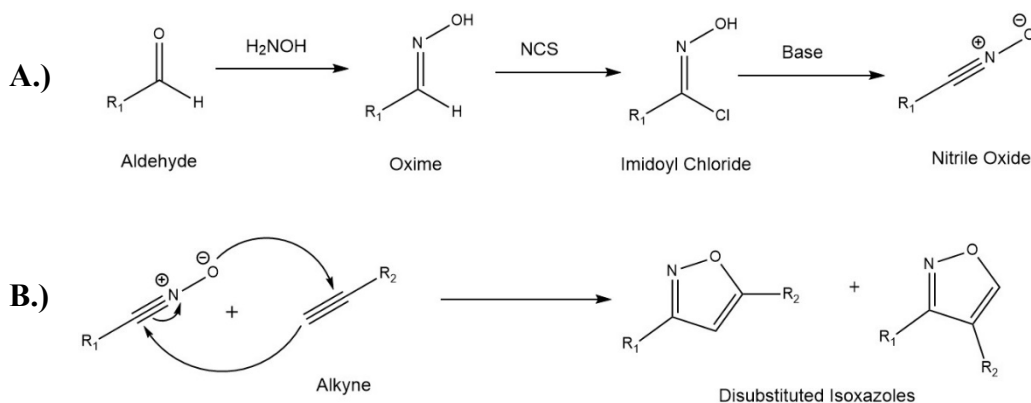


**Figure 7.** Nitrile oxide and alkyne 1,3-dipolar cycloaddition. **A.)** *In situ* generation of the nitrile oxide: The aldehyde is converted to an oxime which reacts with NCS to form the imidoyl chloride. Treatment with base liberates the nitrile oxide *in situ*. **B.)** Addition of an alkyne which results in the 1,3-dipolar cycloaddition.

Another attractive feature of the isoxazole is its stability and potential as a pharmacophore in drug design. This heterocycle can participate in hydrogen bonding interactions as well as  $\pi$ -stacking (16). This reaction has previously seen use in synthesis of modified versions of oligonucleotides and DNA (16, 18) which is shown in **Figure 8**.

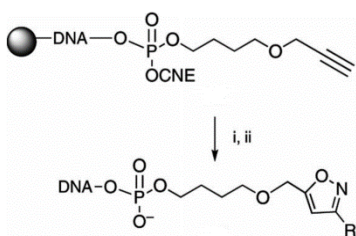


**Figure 8.** Examples of the NOAC reaction being used with DNA. Here is shown an example of the NOAC reaction being used for solid phase modification of oligonucleotides (16). i.) RCHNOH, Chloramine-T monohydrate, NaHCO<sub>3</sub>, EtOH, room temp. ii.) cleavage and deprotection.

The goal of this work is to establish NOAC 1,3-dipolar cycloaddition protocols that can be used to create a stapled peptide. Stapled peptide synthesis with this reaction has not been previously reported. First, a reliable synthetic route to isoxazoles must be found using the NOAC reaction. Once this is established, the amino acids containing the reactive R-groups must be synthesized and then coupled to reinforce the effectiveness of the NOAC protocol. Finally, the amino acids will be incorporated into a peptide which will be exposed to the conditions/reagents previously used to induce the NOAC reaction. At this point, the product should be a stapled  $\alpha$ -helical peptide. An example of what this final product could look like is shown in **Figure 9**.

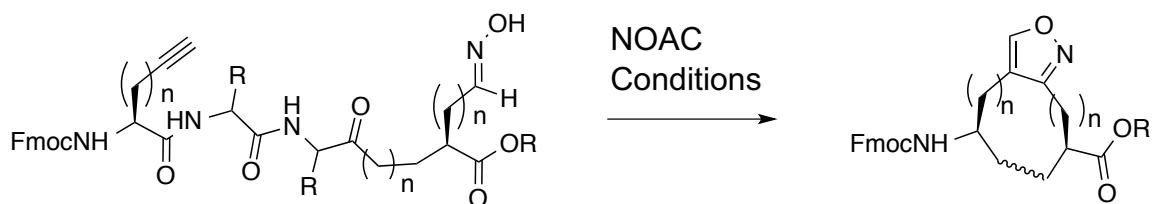


**Figure 9.** Schematic of the final stapled peptide created with the NOAC reaction. In the starting material, note the alkyne group on the left and the oxime on the right. The oxime is generated from an aldehyde.

The primary goal of this work will be attempting 1,3-dipolar cycloaddition reactions with simple substrates. This will allow investigation of reaction conditions and optimization of yields. Simple aldehyde starting materials that will be used include benzaldehyde and phenylacetaldehyde. These substrates will be converted to the corresponding nitrile oxide and then coupled with 1-hexyne, which serves as a simple alkyne substrate. Once these reactions prove successful, the secondary goal will be the synthesis of two unnatural amino acids, one containing an alkyne moiety and another containing an aldehyde moiety. These will then be coupled with some of the previous simple substrates. The alkyne amino acid will be reacted with either benzaldehyde or phenylacetaldehyde derivatives. The aldehyde amino acid will be reacted with 1-hexyne. Subsequently, a cyclization will be attempted between the amino acids themselves to reinforce NOAC protocols. And finally, after cyclization conditions and yields are optimized, the unnatural amino acids will be incorporated into a peptide in one of three orders:  $i, i + 3$ ,  $i, i + 4$ , or  $i, i + 7$ . Solid phase peptide synthesis will be utilized for this. Then, the NOAC conditions will be used to generate the staple and stabilize the  $\alpha$ -helix.

If this could be achieved, it would confirm another synthetic path to generation of hydrocarbon stapled peptides.

## CHAPTER II: MATERIALS AND METHODS

This chapter details the procedures for all syntheses. First, procedures for practice couplings to afford isoxazoles with the simple materials benzaldehyde, phenylacetaldehyde, and 1-hexyne will be described. Next, the procedures for synthesis and protection of unnatural amino acids homopropargyl glycine and aspartic acid  $\beta$ -semialdehyde will be detailed. Finally, procedures for the reactions of these amino acids to afford isoxazoles will be described.

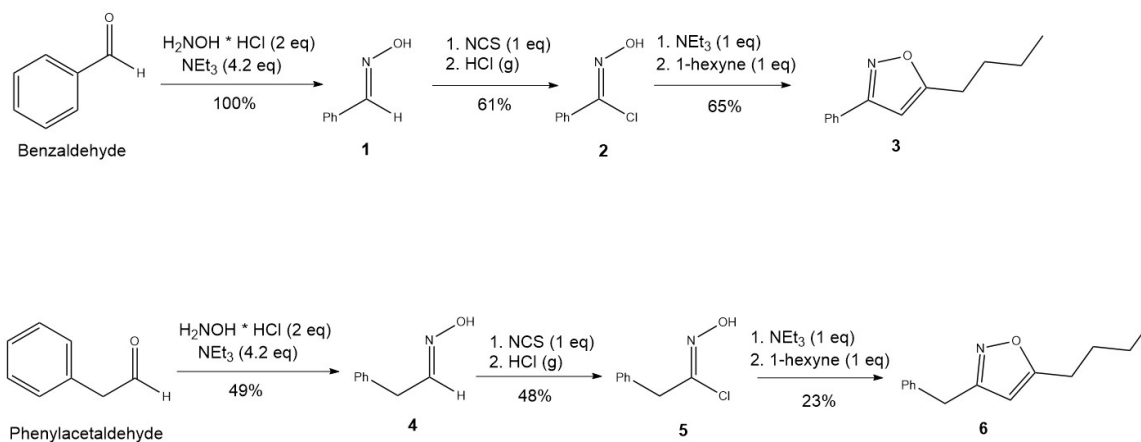
### General Experimental Details

All chemical reagents and solvents were commercially available and used without further purification. Purifications of all products were done on a pre-packed silica gel column using a Teledyne Isco Combiflash system with a UV detector, eluting with a gradient of 100% hexanes to 100% ethyl acetate. Reactions were monitored by analytical thin-layer chromatography (TLC) on silica gel 60 F254 pre-coated on glass plates (Merck). Observation of TLC was conducted by using a UV lamp ( $\lambda_{\text{MAX}} = 254 \text{ nm}$ ) and either ninhydrin or phosphomolybdic acid stain. NMR data were obtained on either a 500 MHz FT-NMR model ECA-500 JEOL or a 300MHz FT-NMR model ECA-300 JEOL (Peabody, MA) purchased with funding provided by the National Science Foundation. Coupling constants (J values) are recorded in hertz (Hz). All signal assignments are based on  $^1\text{H}$ ,  $^{13}\text{C}$ , COSY, HMQC and DEPT<sup>135</sup>. High resolution ESI-MS was performed at Notre Dame University, Notre Dame, Indiana. Ozonolysis was performed with a T-816

Welsbach Ozone Generator (Welsbach Ozone Systems, division of Poylmetrics, Inc., Sunnyvale, CA, U.S.A.).

### Synthesis of Isoxazoles from 1-Hexyne and Simple Aldehydes

The simple aldehydes, benzaldehyde and phenylacetaldehyde, were converted to the corresponding oximes, which were then converted to the hydroximidoyl chloride. Subsequent reaction with base and 1-hexyne afforded isoxazoles. These steps are outlined in **Scheme 1**.



**Scheme 1.** (a) Schematic for synthesis of 5-butyl-3-phenylisoxazole (**4**) and 4-butyl-3-phenylisoxazole (**5**) from benzaldehyde (**1**). (b) Schematic for synthesis of 3-benzyl-5-butylisoxazole (**9**) and 3-benzyl-4-butylisoxazole from phenylacetaldehyde (**6**).

**(E)-Benzaldehyde Oxime (1).** Benzaldehyde (200 mg, 1.9 mmol) was dissolved in 9.4 mL of  $\text{CH}_2\text{Cl}_2$  to create a 0.2 M solution. To this solution was added triethylamine (0.19 mL, 1.9 mmol) and hydroxylamine hydrochloride (261 mg, 3.76 mmol). This was stirred for 20 hours, then poured into a separatory funnel containing 1 M aqueous  $\text{NaHCO}_3$  solution. The product was extracted twice with  $\text{CH}_2\text{Cl}_2$ , then dried with

anhydrous MgSO<sub>4</sub>. After filtration and solvent removal, the crude product was purified *via* Combiflash chromatography eluting with hexanes and ethyl acetate to yield 370 mg of oxime **1** as a clear oil (100%). <sup>1</sup>H NMR (CDCl<sub>3</sub>, 500 MHz): δ 7.38 (m, 3H, aromatic H), 7.57 (m, 2H, aromatic H), 8.15 (s, 1H, oxime H).

**(Z)-N-Hydroxybenzimidoyl Chloride (2).** (*E*)-Benzaldehyde oxime (374 mg, 3.1 mmol) **2** was dissolved in 2.5 mL DMF. To this solution was added approximately one-fifth of the N-chlorosuccinimide (412 mg total, 3.09 mmol). At this point the color of the solution changed from clear to yellow. After about 10 minutes, 5 mL of HCl gas was collected with a syringe from the headspace of a concentrated HCl container and bubbled through the solution. The rest of the NCS was then added in small portions, approximately one-fifth per every five minutes. The solution was then stirred for one hour at room temperature. The imidoyl chloride **2** was purified by pouring the contents of the reaction vessel into water and extracting twice with diethyl ether. The resulting ether layers were then washed three times with water. The organic layers were dried with anhydrous MgSO<sub>4</sub> and filtered. The solvent was removed to afford 294 mg the crude product as a yellow oil (61%). The unstable product was used within one hour in the next synthetic step. <sup>1</sup>H NMR (CDCl<sub>3</sub>, 500 MHz): δ 7.40 (m, 3H, aromatic H), 7.82 (m, 2H, aromatic H). <sup>13</sup>C NMR (CDCl<sub>3</sub>, 125 MHz): δ 127.3, 128.7, 130.9, 132.4, 140.7.

**5-Butyl-3-Phenylisoxazole (3).** (*Z*)-*N*-Hydroxybenzimidoyl chloride (294 mg, 1.9 mmol) **3** was dissolved in 8.0 mL of toluene within one hour of its preparation. To this solution was added triethylamine (0.26 mL, 1.89 mmol). Gas formation was noted upon addition and a precipitate began to form. After stirring for approximately five minutes, 1-hexyne was added to the yellow slurry. The resulting mixture was stirred

overnight at room temperature and then poured into approximately 30 mL of 1M HCl and the product was extracted twice with ethyl acetate. The combined organic layers were dried with anhydrous  $\text{MgSO}_4$ , filtered, and solvent was removed. The crude isoxazole was purified *via* Combiflash chromatography eluting with hexanes and ethyl acetate to yield 249 mg of a clear oil as one isomer (65%).  $^1\text{H}$  NMR ( $\text{CDCl}_3$ , 500 MHz):  $\delta$  0.96 (t, 3H,  $J = 7.45$  Hz, butyl  $\text{CH}_3$ ), 1.42 (m, butyl  $\text{CH}_2$ ), 1.73 (quint, 2H,  $J = 8.02$  Hz, butyl  $\text{CH}_2$ ), 2.79 (t, 2H,  $J = 7.45$  Hz, butyl  $\text{CH}_2$  next to isoxazole), 6.28 (s, 1H, isoxazole H), 7.44 (m, 4H, phenyl H), 7.80 (m, 2H, phenyl H).  $^{13}\text{C}$  NMR ( $\text{CDCl}_3$ , 125 MHz):  $\delta$  13.7 (butyl  $\text{CH}_3$ ), 22.3 (butyl  $\text{CH}_2$ ), 26.6 (butyl  $\text{CH}_2$ ), 29.7 (butyl  $\text{CH}_2$  next to isoxazole), 98.8 (isoxazole H), 126.8 (aromatic H), 128.8 (aromatic H), 128.9 (aromatic H), 129.0 (aromatic H), 129.1 (aromatic H), 156.3 (quaternary C), 162.4 (quaternary C), 174.4 (quaternary C).

**(*E*)-2-Phenylacetaldehyde Oxime (4).** Phenylacetaldehyde (0.58 mL, 5.0 mmol) was dissolved in 25 mL of  $\text{CH}_2\text{Cl}_2$  to create a 0.2 M solution. To this solution was added triethylamine (2.9 mL, 21 mmol) and hydroxylamine hydrochloride (695 mg, 10 mmol). This was stirred for 24 hours, then poured into a separatory funnel containing 1 M aqueous  $\text{NaHCO}_3$  solution. The product was extracted twice with  $\text{CH}_2\text{Cl}_2$ , then dried with anhydrous  $\text{MgSO}_4$ . After filtration and solvent removal, 335 mg of crude oxime **4** remained as a clear oil (49%).  $^1\text{H}$  NMR ( $\text{CDCl}_3$ , 500 MHz):  $\delta$  3.53 (d, 2H,  $J = 6.19$ ,  $\text{CH}_2$  next to oxime), 3.74 (d, 2H,  $J = 5.50$ ), 6.90 (t, 1H,  $J = 5.50$ , oxime H), 7.30 (m, 12 H, aromatic H), 7.54 (t, 2H,  $J = 6.19$  Hz, aromatic H).

**(*Z*)-*N*-Hydroxy-2-Phenylacetimidoyl Chloride (5).** (*E*)-2-Phenylacetaldehyde oxime (335 mg, 2.5 mmol) **5** was dissolved in 2.1 mL of DMF. To this solution was

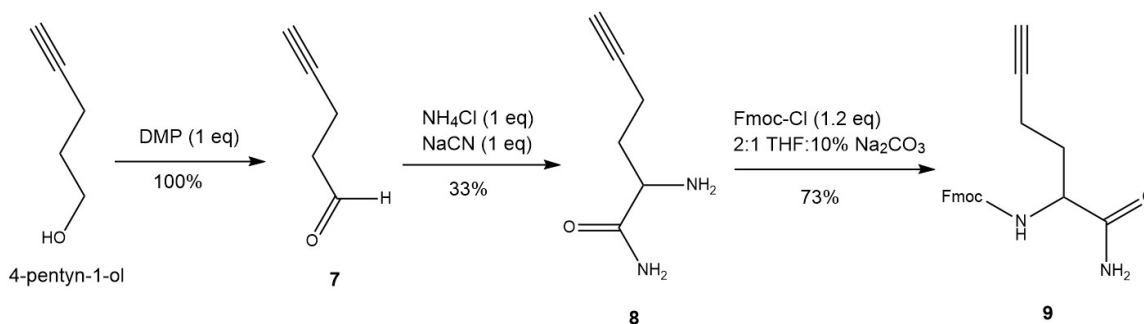
added approximately one-fifth of the N-chlorosuccinimide (331 mg, 2.5 mmol). No color change was noted. After about 10 minutes, 4 mL of HCl gas was collected with a syringe from the headspace of a concentrated HCl container and bubbled through the solution. At this point, the color of the solution changed from clear to blue. The rest of the NCS was then added in small portions, approximately one-fifth per every five minutes. The blue color faded over time and the solution became yellow. The yellow color also slowly faded. The solution was then stirred for one hour at room temperature after the last addition of NCS. The crude imidoyl chloride **5** was purified by pouring the contents of the reaction vessel into water and extracting twice with diethyl ether. The resulting ether layers were then washed three times with water. The organic layers were dried with anhydrous MgSO<sub>4</sub> and then the solvent was removed to afford 204 mg of the crude product as a yellow oil (48%). The unstable product was used for the next synthetic step within one hour of its preparation. <sup>1</sup>H NMR (CDCl<sub>3</sub>, 500 MHz): δ 3.81 (s, 2H, CH<sub>2</sub>), 7.28 (m, 7H, aromatic H), 8.15 (s, 1H, aromatic H). <sup>13</sup>C NMR (CDCl<sub>3</sub>, 125 MHz): δ 41.8 (CH<sub>2</sub>), 126.5, 127.7, 128.1, 165.9.

**3-Benzyl-5-butyloxazole (6).** (*Z*)-*N*-Hydroxy-2-Phenylacetimidoyl chloride (204 mg, 1.2 mmol) **5** was dissolved in 5.0 mL of toluene within one hour of its preparation. To this solution was added triethylamine (0.17 mL, 1.20 mmol). No gas formation was noted upon addition, but the initial light-yellow color changed to lime green and a solid precipitate was noted. The slurry eventually became dark yellow. After stirring for approximately five minutes, 1-hexyne (0.14 mL, 1.20 mmol) was added to the slurry. This was stirred overnight at room temperature. The following day, the flask contents were poured into approximately 30 mL of 1M HCl and the product was

extracted twice with ethyl acetate. The fractions were dried with anhydrous  $\text{MgSO}_4$  and solvent was removed. The crude isoxazole was purified *via* Combiflash chromatography eluting with hexanes and ethyl acetate to yield the product as 60 mg of yellow oil (23%).  $^1\text{H}$  NMR ( $\text{CDCl}_3$ , 500 MHz):  $\delta$  0.92 (t, 3H,  $J = 7.22$ , butyl  $\text{CH}_3$ ), 1.35 (sextet, 2H,  $J = 7.22$ , butyl  $\text{CH}_2$ ), 1.63 (quint, 2H,  $J = 7.57$ , butyl  $\text{CH}_2$ ), 2.67 (t, 2H,  $J = 7.91$ , butyl  $\text{CH}_2$  next to isoxazole), 5.73 (s, 1H, isoxazole H), 7.23 (m, 5H, phenyl H), 7.29 (m, 2H, phenyl H).  $^{13}\text{C}$  NMR ( $\text{CDCl}_3$ , 125 MHz):  $\delta$  13.8 (butyl  $\text{CH}_3$ ), 22.3 (butyl  $\text{CH}_2$ ), 26.5 (butyl  $\text{CH}_2$ ), 29.6 (butyl  $\text{CH}_2$ ), 32.6 ( $\text{CH}_2$  between isoxazole and phenyl), 100.7 (isoxazole H), 126.8 (aromatic H), 128.8 (aromatic H), 128.9 (aromatic H), 137.8 (quaternary C), 163.0 (quaternary C), 173.8 (quaternary C).

### Synthesis of Alkyne and Aldehyde Amino Acids

The protected alkyne amino acid was obtained in three steps, which are detailed in **Scheme 2**, from 4-pentyn-1-ol. The aldehyde amino acid was obtained in two steps, detailed in **Scheme 3**, from Fmoc-L-allylglycine.



**Scheme 2.** Schematic for synthesis of homopropargyl glycine.

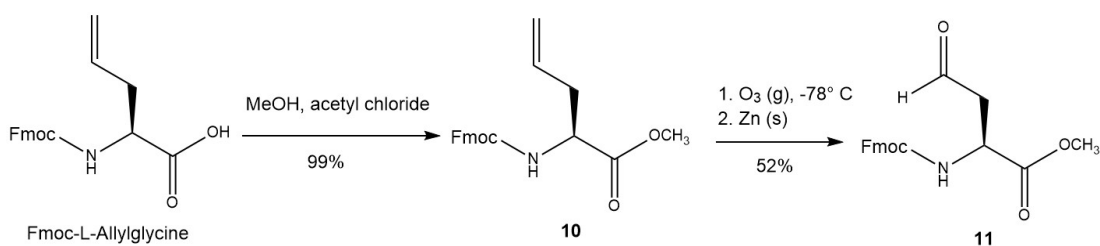
**4-Pentyn-1-al (7).** 4-Pentyn-1-ol (336 mg, 4.0 mmol) was dissolved in 20 mL  $\text{CH}_2\text{Cl}_2$ , and DMP (1.696 g, 4.0 mmol) was added. Then, 25 mL  $\text{CH}_2\text{Cl}_2$  was loaded into

an addition funnel and 2 drops of water were added and mixed thoroughly with a pipette. This mixture was added slowly to the reaction vessel over approximately 30 mins. The reaction was stirred for an additional 1.5 hours. Approximately 15 mL  $\text{CH}_2\text{Cl}_2$  was removed, then 20 mL diethyl ether was added to the reaction vessel. It was then evaporated until approximately 5 mL of solvent remained. This was diluted with approx. 40 mL diethyl ether and washed with 30 mL of a 1:1 solution of  $\text{NaHCO}_3$ :10%  $\text{Na}_2\text{S}_2\text{O}_3$ . The organic layer was washed once with water and once with brine, and then the combined aqueous layers were back extracted once with another 40 mL of diethyl ether. The combined organic layers were washed once more with both water and brine and then dried with anhydrous  $\text{MgSO}_4$  and filtered. Most of the solvent was removed. Due to the potential volatility of the product, the temperature of the water bath during solvent removal was kept at approximately  $40^\circ\text{C}$  and the clear liquid was evaporated until its weight was equivalent to the theoretical yield for the aldehyde. This afforded crude 4-pentyn-1-al as a clear liquid (100%).  $^1\text{H}$  NMR ( $\text{CDCl}_3$ , 500 MHz):  $\delta$  1.20 (t, 1H,  $J = 7.57$  Hz), 1.78 (quint, 2H,  $J = 6.59$  Hz), 1.98 (m, 2H), 2.33 (m, 2H), 2.51 (m, 2H), 2.69 (t, 2H,  $J = 6.87$  Hz), 3.46 (q, 1H,  $J = 6.87$  Hz), 3.77 (t, 2H,  $J = 6.30$  Hz), 9.80 (s, 1H, aldehyde H).

**2-Aminohex-5-ynamide (8).** 4-pentyn-1-al (328 mg, 4.0 mmol) was dissolved in 10 mL of approximately 15%  $\text{NH}_4\text{OH}$  (aq) solution.  $\text{NH}_4\text{Cl}$  (214 mg, 4.0 mmol) was added. Afterwards,  $\text{NaCN}$  (196 mg, 4.0 mmol) was added, and the solution was stirred overnight at  $40^\circ\text{C}$  in a sand bath. After approximately 18 hours, the contents of the reaction vessel were diluted with 40 mL of water. The product was extracted from this twice with ethyl acetate. The organic layers were dried with anhydrous  $\text{MgSO}_4$ . After

filtration and solvent removal, what remained was 145 mg of the crude product **8** as a clear oil (33%). Note: the intermediate nitrile was hydrolyzed to an amide.  $^1\text{H}$  NMR ( $\text{CDCl}_3$ , 500 MHz):  $\delta$  1.78 (sextet, 1H,  $J = 6.87$  Hz), 2.00 (m, 2H), 2.12 (s, 1H, alkyne H), 2.32 (3H), 3.75 (t, 1H,  $J = 6.30$  Hz).  $^{13}\text{C}$  NMR ( $\text{CDCl}_3$ , 125 MHz):  $\delta$  15.0 ( $\text{CH}_2$  next to alkyne), 31.1 ( $\text{CH}_2$  next to amine), 61.3 (amine C), 68.9 (Alkyne quaternary C), 70.3 (should not be present), 81.8, 84.0 (Terminal C of alkyne), 165.9 (Amide  $\text{C}=\text{O}$ ).

**9H-fluoren-9-yl (1-amino-1-oxohex-5-yn-2-yl) carbamate (N-protection of 2-Aminohex-5-ynamide) (9).** The amide derivative **3** (145 mg, 1.1 mmol) was dissolved in 6.6 mL THF. 3.3 mL of aqueous  $\text{Na}_2\text{CO}_3$  was added. Fmoc-Cl (346 mg, 1.3 mmol) was added to create a yellow solution, which was stirred overnight at room temperature. After approximately 22 hours, a white solid was noted at the bottom of the flask. The contents of the flask were diluted with 40 mL of water, and the product was extracted twice with 40 mL of ethyl acetate. The organic layers were dried with anhydrous  $\text{MgSO}_4$ , filtered, and solvent was removed. A crude NMR was obtained and then the protected amide derivative **9** was purified *via* Combiflash chromatography eluting with hexanes and ethyl acetate to yield 243 mg of the product as a pink oil (73%).  $^1\text{H}$  NMR ( $\text{CDCl}_3$ , 500 MHz):  $\delta$  0.92 (m, 1H), 1.28 (m, 2H), 4.01 (d, 1H,  $J = 5.73$  Hz), 7.32 (t, 2H,  $J = 7.45$  Hz, Fmoc aromatic H), 7.40 (m, 2H, Fmoc aromatic H), 7.60 (m, 2H, Fmoc aromatic H), 7.77 (m, 2H, Fmoc aromatic H).  $^{13}\text{C}$  NMR ( $\text{CDCl}_3$ , 125 MHz):  $\delta$  14.0 ( $\text{CH}_2$  next to alkyne), 14.7, 22.6, 31.7 (Fmoc CH), 46.9 (Fmoc  $\text{CH}_2$ ), 50.4 ( $\alpha$ -C), 64.9 (Alkyne quaternary C), 119.9, 124.6, 124.8, 127.0, 127.5, 141.4, 144.3, 165.9 (Amide  $\text{C}=\text{O}$ ).



**Scheme 3.** Schematic for synthesis of aspartic acid  $\beta$ -semialdehyde.

**Fmoc-L-Allylglycine  $\alpha$ -Methyl Ester (10).** Fmoc-L-allylglycine (1.00 g, 3.0 mmol) was dissolved in 50 mL of MeOH. Acetyl chloride (5 drops) was added to the solution and it was stirred at ambient temperature for approximately 72 hours. No color change was noted. The excess MeOH was evaporated until approximately 5 mL of solvent remained. The remaining liquid was diluted with approximately 70 mL of ethyl acetate and then washed once with approximately 50 mL of 1M  $\text{NaHCO}_3$ . The resulting organic layer was dried with  $\text{MgSO}_4$ , filtered, and solvent was removed to yield 994 mg of crude Fmoc-L-allylglycine  $\alpha$ -methyl ester (**2**) as a white, waxy solid (99%).  $^1\text{H}$  NMR ( $\text{CDCl}_3$ , 500 MHz):  $\delta$  2.52 (m, 1H), 2.58 (m, 1H), 3.74 (s, 3H,  $\text{OCH}_3$ ), 4.23 (t, 1H,  $J = 7.45$  Hz), 4.38 (m, 1H), 4.40 (m, 1H), 5.13 (m, 1H, vinyl H), 5.39 (d, 1H,  $J = 8.02$  Hz, vinyl H), 7.30 (t, 2H,  $J = 7.45$  Hz, Fmoc H), 7.38 (t, 2H,  $J = 7.45$  Hz, Fmoc H), 7.58 (m, 2H, Fmoc H), 7.76 (d, 2H,  $J = 8.02$  Hz, Fmoc H).  $^{13}\text{C}$  NMR ( $\text{CDCl}_3$ , 125 MHz):  $\delta$  14.3, 36.8, 47.3, 52.5, 53.4, 60.5, 67.2, 119.5, 120.1, 125.2, 127.2, 127.8, 132.2, 141.4, 143.9, 144.0, 155.8, 165.9, 172.3 (Ester  $\text{C}=\text{O}$ ).

**Fmoc-L-Aspartic Acid  $\beta$ -Semialdehyde  $\alpha$ -Methyl Ester (11).** Fmoc-L-allylglycine  $\alpha$ -methyl ester (500 mg, 1.4 mmol) **10** was dissolved in approximately 150 mL of  $\text{CH}_2\text{Cl}_2$  and stirred. For approximately 10 minutes,  $\text{O}_2$  (g) was bubbled through the

solution while it was being cooled to  $-78^{\circ}\text{C}$ . Then, the ozonizer was turned on for approximately 10 minutes. Due to perceived technical issues, the ozonizer was turned off before the characteristic blue color was achieved and the solution was still clear. Solid zinc metal (300 mg, 4.6 mmol) was immediately added and the solution was stirred for one hour. The contents of the flask were poured into a separatory funnel and washed once with water. The remaining zinc was discarded. The resulting organic layer was dried with  $\text{MgSO}_4$ , filtered, and the solvent removed. The crude aldehyde was purified *via* Combiflash chromatography eluting with hexanes and ethyl acetate to yield 255 mg of the product **11** as a clear oil (52%).  $^1\text{H}$  NMR ( $\text{CDCl}_3$ , 300 MHz):  $\delta$  3.07 (m, 2H), 3.75 (s, 7H,  $\text{OCH}_3$  ester), 4.21 (t, 2H,  $J = 6.88$  Hz), 4.38 (m, 5H), 4.66 (m, 2H), 5.80 (d, 3H,  $J = 7.91$  Hz), 7.31 (m, 10H, Fmoc H), 7.56 (d, 5H,  $J = 6.88$  Hz, Fmoc H), 7.74 (d, 5H,  $J = 7.22$  Hz, Fmoc H), 9.71 (s, 1H, aldehyde H).  $^{13}\text{C}$  NMR ( $\text{CDCl}_3$ , 125 MHz):  $\delta$  47.2, 53.0, 53.6, 67.4, 120.1, 124.9, 125.2, 127.2, 127.9, 141.4, 143.7, 143.9, 156.1, 171.3 (Ester  $\text{C}=\text{O}$ ), 199.5 (Aldehyde  $\text{C}=\text{O}$ ).

### CHAPTER III: RESULTS AND DISCUSSION

The primary goal of establishing an effective synthesis of isoxazoles was pursued. The most effective route proved to be a three-step synthesis starting from an aldehyde. The aldehyde was converted to an oxime, which was then converted to the corresponding hydroximidoyl chloride. Oxime formation was achieved with a procedure from Kieta, Vandamme, and Paquin (20). Hydroximidoyl chlorides were prepared with NCS as a chlorinating agent, following a procedure from Liu, Shelton, and Howe (21). The hydroximidoyl chloride was then reacted with base to liberate the nitrile oxide, and shortly after, the alkyne was added to afford the isoxazole *via* a 1,3-dipolar cycloaddition.

These procedures afforded isoxazoles with both benzaldehyde and phenylacetaldehyde precursors. One regioisomer of the isoxazole was present, but no analysis was performed to determine whether the 3,5-disubstituted or 3,4-disubstituted isomer was obtained. Literature suggests that the 3,5-disubstituted isomer should be the predominant isomer. However, isoxazoles are not the only product that can form. Nitrile oxides can undergo dimerization to 1,2,5-oxadiazole-2-oxides, which are commonly known as furoxans (22). This mechanism is shown below in **Figure 10**. While no furoxans were definitively isolated from the attempted cyclizations, the presence of aromatic, later-eluting side products was noted.

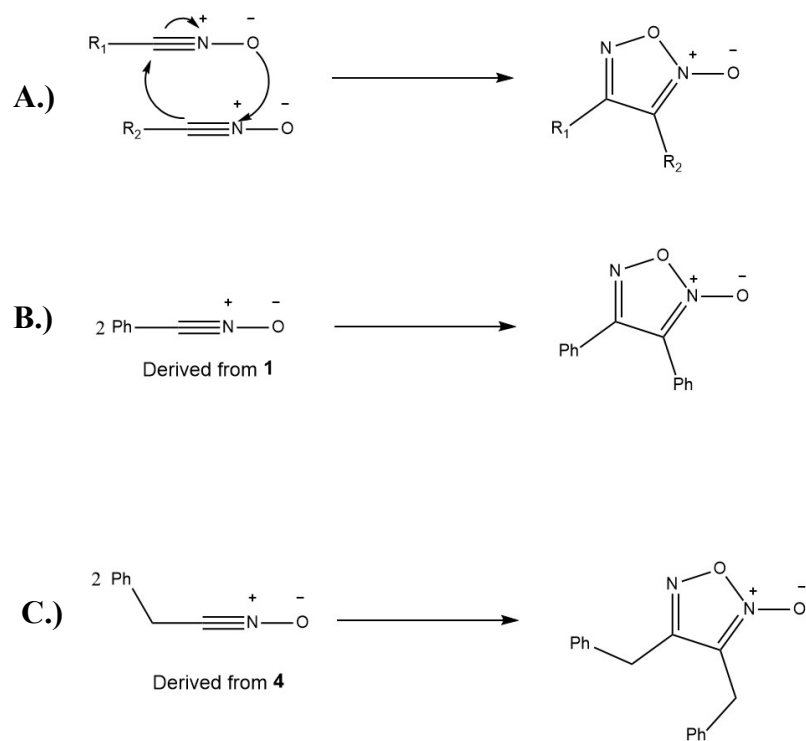


**Figure 10.** Mechanism and examples of nitrile oxide dimerization to furoxans (22). **A.)** Dimerization mechanism. **B.)** Example of furoxan formation from **1**. **C.)** Example of furoxan formation from **4**.

(*Z*)-*N*-Hydroxybenzimidoyl chloride showed poor stability after isolation. Yields from 1,3-dipolar cycloaddition attempts with 1-hexyne and (*Z*)-*N*-hydroxybenzimidoyl chloride decreased as the time between isolation of the imidoyl chloride and the beginning of the cyclization increased. Initially, the procedure for synthesis of 5-butyl-3-phenylisoxazole was carried out with (*Z*)-*N*-hydroxybenzimidoyl chloride that was 24 hours old, resulting in a yield of 34%. Subsequent attempts to increase this yield included slow addition of triethylamine and the use of a Cu(I) catalyst. Slow addition of triethylamine was attempted to keep the nitrile oxide concentration low and prevent dimerization to furoxans. Both this method and the utilization of Cu(I) resulted in poor yields (17-18%), but both attempts also included (*Z*)-*N*-hydroxybenzimidoyl chloride that had been stored in the refrigerator, but was greater than 24 hours old. When attempting the original procedure with fresh (less than one hour old) (*Z*)-*N*-hydroxybenzimidoyl chloride, a much higher yield (65%) was observed for 5-butyl-3 phenylisoxazole. This procedure was also utilized in the synthesis of 3-benzyl-5-butylisoxazole, but high yields were not obtained, indicating that immediate use of the hydroximidoyl chloride may not be the only factor that determines the efficiency of the reaction. A summary of conditions attempted is shown below in **Table 1**. Further investigation is needed to determine the relationship between the hydroximidoyl chloride age and the efficiency of the reaction; Furthermore, this technique could be combined with other methods such as slow base addition. Alternative storage methods besides refrigeration for the hydroximidoyl chloride could also be attempted to decrease its decomposition rate.

<b>Table 1. Conditions, Hydroximidoyl Chloride Age, and Percent Yields for Cyclization Attempts with 1-Hexyne</b>			
Aldehyde Starting Material	Conditions (Solvent, base, time, temp, catalyst)	Hydroximidoyl Chloride Age (hr)	% Yield
Benzaldehyde	Toluene, NEt <sub>3</sub> , 24 hrs, room temp, no catalyst	24	34%
Benzaldehyde	Toluene, NEt <sub>3</sub> (slow addition), 24 hrs, room temp, no catalyst	72	17%
Benzaldehyde	1:1 tBuOH:H <sub>2</sub> O, NEt <sub>3</sub> , 24 hrs, room temp, CuSO <sub>4</sub> catalyst	Two weeks	18%
Benzaldehyde	Toluene, NEt <sub>3</sub> , 24 hrs, room temp, no catalyst	<1	65%
Phenylacetaldehyde	Toluene, NEt <sub>3</sub> , 24 hrs, room temp, no catalyst	<1	23%

Once a synthetic path to isoxazoles was established, the secondary goal of synthesizing unnatural amino acids was achieved. The amino acid with the alkyne substituent, homopropargylglycine, was made from 4-pentyn-1-ol following a procedure reported by Dong, Merkel, Moroder, and Budisa (23). The procedure is a Strecker synthesis, which is a well-established process for synthesis of unnatural amino acids. In the Strecker synthesis, an aldehyde is converted to an  $\alpha$ -amino nitrile, which is subsequently hydrolyzed to afford an  $\alpha$ -amino acid (23). Oxidation of 4-pentyn-1-ol with DMP proceeded smoothly to afford the aldehyde **9**. However, the expected nitrile that

should have been obtained from the reaction of the aldehyde with NaCN and NH<sub>4</sub>Cl hydrolyzed to the amide derivative **10**. The predicted mechanism for this step is shown below in **Figure 11**. This resulting amide derivative was successfully protected with Fmoc-Cl to afford a protected amino acid alkyne.

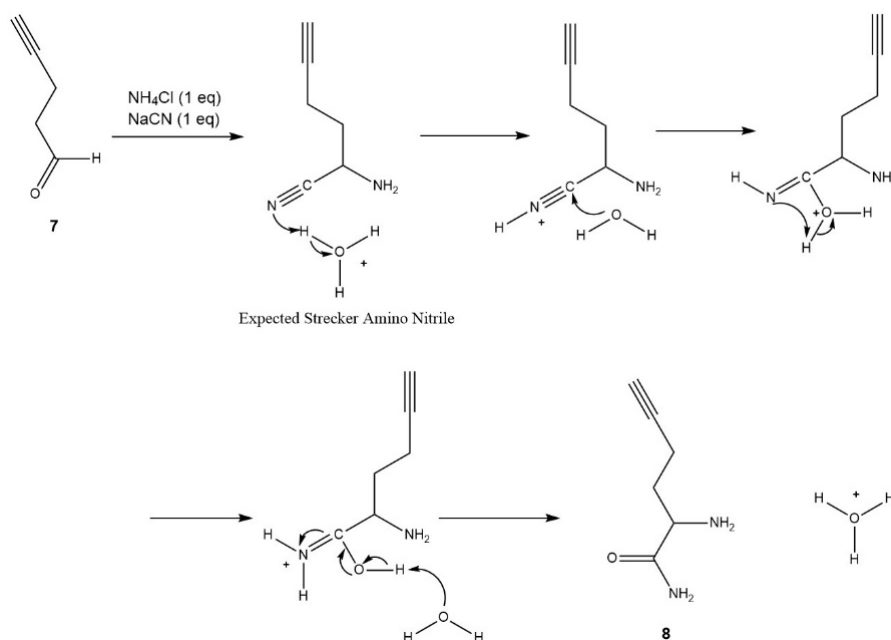
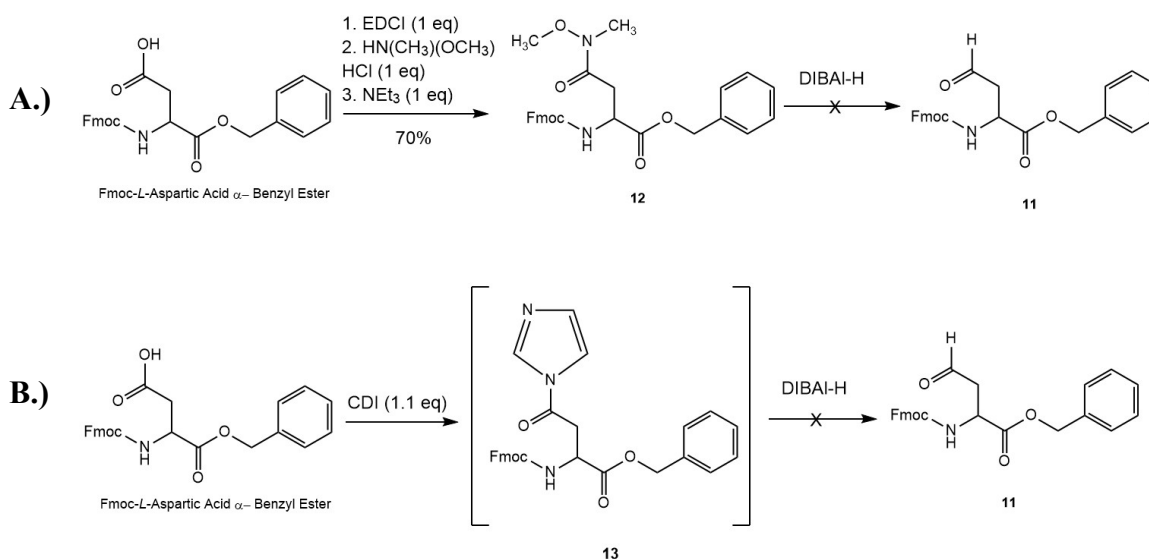


**Figure 11.** Proposed mechanism of acid catalyzed hydrolysis of the expected nitrile product.

Several paths to an aldehyde amino acid were pursued. First, a procedure reported by Roberts, Morris, Dobson, and Gerrard was attempted (24). This procedure involved conversion of aspartic acid to the corresponding Weinreb amide and subsequent reduction to afford an aldehyde with DIBAL-H. Aspartic acid was successfully converted to the corresponding Weinreb amide. However, subsequent attempts to reduce the Weinreb amide with DIBAL-H were unsuccessful. Anywhere from 1.5 to 2.0 molar equivalents of DIBAL-H was used in temperatures ranging from -78°C to ambient

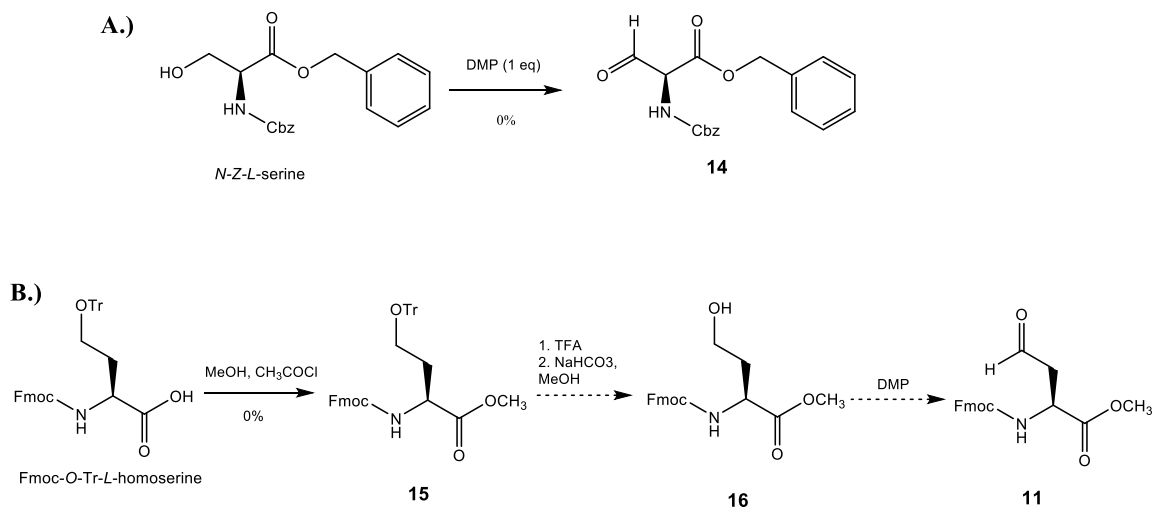
temperature. After failure to reduce the Weinreb amide, another reduction procedure reported by Ivkovic, Lembacher-Fadum, and Breinbaur was attempted (25). This procedure described the use of CDI to react with a carboxylic acid to generate a reactive intermediate, which was subsequently reduced to an aldehyde with DIBAL-H. This was also unsuccessful. A summary of these attempts is shown in **Scheme 4**.



**Scheme 4.** Reduction attempts to achieve the desired aldehyde. **A.)** Conversion of aspartic acid to a Weinreb amide, then attempted reduction with DIBAL-H. **B.)** *In situ* generation of the imidazole intermediate from aspartic acid with CDI and subsequent reduction attempt with DIBAL-H.

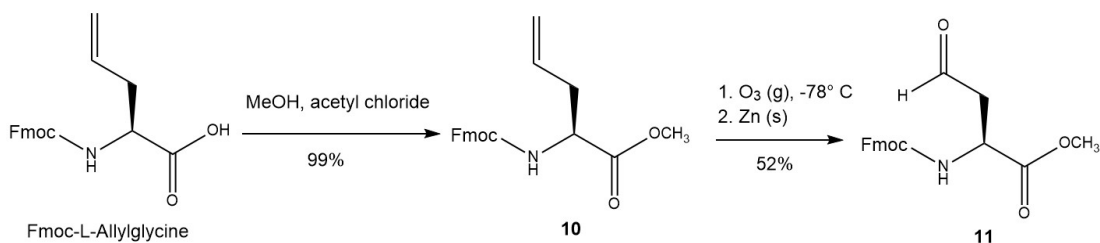
Another approach to an aldehyde amino acid is oxidation of an amino acid alcohol. First, oxidation of *N-Z-L* serine benzyl ester was attempted utilizing DMP, but this proved unsuccessful. Another option is oxidation of homoserine. Fmoc-*O*-trityl-*L*-homoserine was obtained and *O*-protection was attempted. The initial protection step,

which was conversion to a methyl ester, proved unsuccessful and a white precipitate formed in the bottom of the flask. This precipitate was insoluble in organic solvents and therefore could not be purified. The small amount of organic-soluble material that was obtained did not contain the amino acid. A summary of both oxidation attempts is shown below in **Scheme 5**.



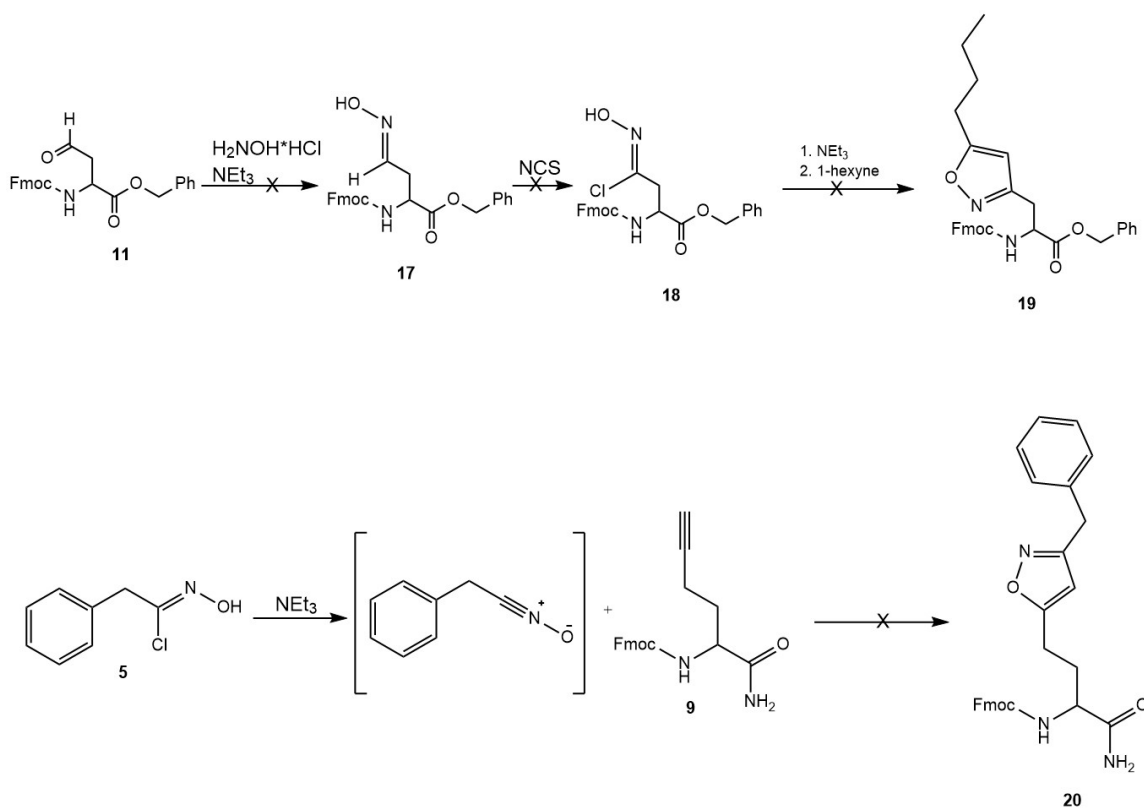
**Scheme 5.** Attempted oxidation reactions with amino acid alcohols. **A.)** Attempted oxidation of *N*-Z-*L*-serine. **B.)** Attempted *O*-protection of Fmoc-*O*-Tr-*L*-homoserine.

Finally, the aldehyde amino acid, Fmoc-*L*-aspartic acid  $\beta$ -semialdehyde  $\alpha$ -methyl ester, was successfully made with a two-step synthesis from Tudor, Lewis, and Robins involving ozonolysis of an alkene (**26**). Fmoc-*L*-allylglycine was first protected as the methyl ester. Subsequently, ozonolysis was performed to afford the aldehyde. Due to technical issues with the ozone generator, yields were lower than expected. **Scheme 6** details the successful route to the aldehyde amino acid.



**Scheme 6.** Successful synthesis of Fmoc-*L*-aspartic acid  $\beta$ -semialdehyde. Esterification of allylglycine is followed by ozonolysis to afford the aldehyde.

The amino acids proved to be incapable of undergoing the reactions of isoxazole formation. Aspartic acid  $\beta$ -semialdehyde was not successfully converted to its corresponding oxime with convincing NMR data. Subsequent attempt at conversion to the hydroximidoyl chloride and the cyclization attempt with 1-hexyne were both unsuccessful, possibly due to incomplete ozonolysis and impurity of the aldehyde product. The protected amide derivative of homopropargyl glycine was combined with (*Z*)-*N*-hydroxy-2-Phenylacetimidoyl chloride in an attempt to generate the corresponding isoxazole, which was also unsuccessful. A summary of these attempts is shown in **Scheme 7**.



**Scheme 7.** Failed cyclization attempts with unnatural amino acids. **A.)** Failed conversion of the aldehyde amino acid to oxime, hydroximidoyl chloride, and subsequent failed reaction with 1-hexyne. **B.)** Failed reaction of **5** with the alkyne amino acid and base to afford an isoxazole.

## Conclusion

With all results considered, much work remains to achieve the final desired product. More cyclization attempts with varied starting materials should be performed to confirm efficiency of the nitrile oxide-alkyne cycloaddition reaction and optimize yields of isoxazole. Yield optimization is crucial for the final peptide synthesis and stapling. Once yields are consistently high and procedures for the synthesis of isoxazoles are

optimized, characterization of isomers is another priority. While one isomer was isolated from the attempts in this work, two regioisomers may be present. Literature suggests that the 3,5-disubstituted isomer should predominate (16), but this should be confirmed for the reactions in this work. Furthermore, characterization of potential side products should be performed to understand what else is being formed during cyclizations. Finally, once these problems are solved, the final goal of producing a peptide can be pursued. The unnatural amino acids should be incorporated into a peptide with solid phase Fmoc peptide synthesis. Once this is achieved, the peptide will be exposed to the optimized conditions for formation of the oxime, hydroximidoyl chloride, and finally the isoxazole.

## REFERENCES

1. Santos, R.; Ursu, O.; Gaulton, A.; Bento, A. P.; Donadi, R. S.; Bologa, C. G.; Karlsson, A.; Al-Lazikani, B.; Hersey, A.; Oprea, T. I.; Overington, J. P. "A comprehensive map of molecular drug targets." *Nature Reviews Drug Discovery*. **2017**, *16*, 19-34.
2. Bissantz, Caterina; Khun, Bernd; Stahl, Martin. "A Medicinal Chemist's Guide to Molecular Interactions." *J. Med. Chem.* **2010**, *53*, 5061-5084.
3. Tonge, Peter J. "Drug-Target Kinetics in Drug Discovery." *ACS Chem. Neurosci.* **2018**, *9*, 29-39.
4. Gonzalez, Mileidy W.; Cann, Maricel G. "Protein Interactions and Disease." *PLoS Comput. Biol.* **2012**, *8*.
5. Berg, L.; Mishra, B.K.; Andersson, C.D.; Ekstrom, F.; Linusson, A. The Nature of Activated Non-Classical Hydrogen Bonds: A Case Study on Acetylcholinesterase-Ligand Complexes. *Chemistry*. **2016**, *22*, 2672.
6. Zelekin, Alexander N.; Ehrhardt, Carston; Healy, Anne Marie. "Materials and methods for delivery of biological drugs." *Nature Chemistry*. **2016**, *8*, 997-1007.
7. 6. Cromm, P. M.; Spiegel, J.; Grossmann, T. M. "Hydrocarbon Stapled Peptides as Modulators of Biological Function." *ACS Chemical Biology*. **2015**, *10*, 1358-1361.
8. Milroy, Lech-Gustav; Grossman, Tom M.; Hennig, Sven; Brunsveld, Luc; Ottmann Christian. "Modulators of Protein-Protein Interactions." *Chem. Rev.* **2014**, *114*, 4695-4748.

9. Klein, M. A. "Stabilized helical peptides: a strategy to target protein–protein interactions." *ACS Medicinal Chemistry Letters*. **2014**, 5, 838-839.
10. Cistrone, Philip A.; Silvestri, Anthony P.; Hintzen, Jordi C. J.; Dawson, Philip E. "Rigid Peptide Macrocycles from On-Resin Glaser Stapling." *ChemBioChem*. **2018**, 19, 1031-1045.
11. Shin, Min-Kyung; Hyun, Yu-Jung; Li, Ji Hoon; Lim, Hyun-Suk. "Comparison of Cell Permeability of Cyclic Peptoids and Linear Peptoids." *ACS Combi. Sci*. **2018**, 20, 237-242.
12. Jayatunga, Madura K. P.; Thompson, Sam; Hamilton, Andrew D. "α-Helix Mimetics: Outwards and Upwards." *Bioorg. Med. Chem. Lett*. **2014**, 24, 717-724.
13. Blackwell, Helen E.; Grubbs, Robert H. "Highly Efficient Synthesis of Covalently Cross-Linked Peptide Helices by Ring-Closing Metathesis." *Angew. Chem. Int. Ed*. **1998**, 37, 3281-3283.
14. Kim, Young-Woo; Katchukian, Peter S.; Verdine, Gregory L. "Introduction of All-Hydrocarbon *i, i*+3 Staples to α-Helices Via Ring-Closing Olefin Metathesis." *Org. Lett*. **2010**, 12, 3046-3049.
15. Walensky, Loren D.; Kung, Andrew L.; Escher, Iris; Malia, Thomas J.; Barbuto, Scott; Wright, Renee D.; Wagner, Gerhard; Verdine, Gregory L.; Korsmeyer, Stanley J. "Activation of Apoptosis in Vivo by a Hydrocarbon-Stapled BH3 Helix." *Science*. **2004**, 305, 1466-1470.
16. Heaney, Frances. "Nitrile Oxide/Alkyne Cycloadditions – A Credible Platform for Synthesis of Bioinspired Molecules by Metal-Free Molecular Clicking." *Eur. J. Org. Chem*. **2012**, 3043-3058.
17. Amblard, Franck; Cho, Jong Hyun; Schinazi, Raymond F. "Cu(I)-Catalyzed Huisgen Azide-Alkyne 1,3-Dipolar Cycloaddition Reaction in Nucleoside, Nucleotide, and Oligonucleotide Chemistry." *Chem. Rev*. **2009**, 109, 4207-4220.
18. Krell, Katja; Harijan, Dennis; Ganz, Dorothee; Doll, Larissa; Wagenknecht, Hans-Achim. "Postsynthetic Modifications of DNA and RNA by Means of Copper-Free Cycloadditions as Bioorthogonal Reactions" *Bioconjugate Chem*. **2020**, 31, 990-1011.
19. Yu, Zhi-Xiang; Carmella, Pierluigi; Houk, K. N. "Dimerizations of Nitrile Oxides to Furoxans Are Stepwise via Dinitrosoalkene Diradicals: A Density Functional Theory Study" *J. Am. Chem. Soc*. **2003**, 125, 15420-15425.
20. Keita, Massaba; Vandamme, Mathilde; Paquin, Jean-François. "Synthesis of Nitriles and Primary Amides Using XtalFluor-E." *Synthesis*. **2015**, 47, 3758-3766.

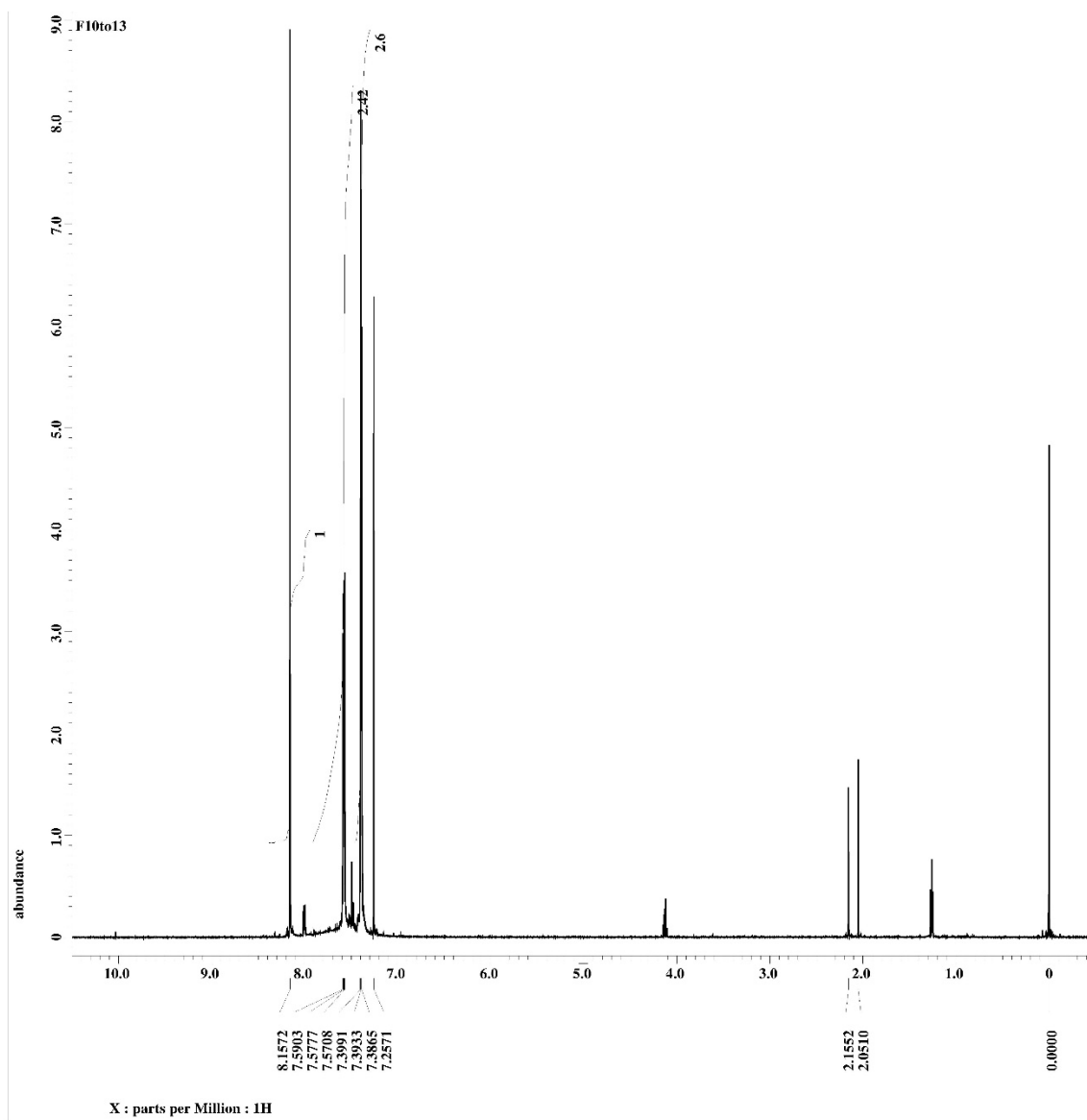
21. Liu, Kou-Chang; Shelton, Becky R.; Howe, Robert K. "A Particularly Convenient Preparation of Benzohydroximinoyl Chlorides (Nitrile Oxide Precursors)." *J. Org. Chem.* **1980**, *45*, 3916-3918.
22. Yu, Zhi-Xiang; Caramella, Pierluigi; Houk, K. N. "Dimerizations of Nitrile Oxides to Furoxans Are Stepwise via Dinitrosoalkene Diradicals: A Density Functional Theory Study." *J. Am. Chem. Soc.* **2003**, *125*, 15420-15425.
23. Dong, Shouliang; Merkel, Lars; Moroder, Luis; Budisa, Nediljko. "Convenient Syntheses of Homopropargylglycine." *J. Pept. Sci.* **2008**, *14*, 1148-1150.
24. Roberts, Sarah J.; Morris, Jonathan C.; Dobson, Renwick C. J.; Gerrard, Juliet A. "The Preparation of (S)-Aspartate Semi-Aldehyde Appropriate for Use in Biochemical Studies." *Bioorg. Med. Chem. Lett.* **2003**, *13*, 265-267.
25. Ivkovic, Jakov; Lembacher-Fadum, Christian; Breinbauer, Rolf. "A Rapid and Efficient One-Pot Method for the Reduction of N-Protected  $\alpha$ -Amino Acids to Chiral  $\alpha$ -Amino Aldehydes Using CDI/DIBAL-H." *Org. Biomol. Chem.* **2015**, *13*, 10456-10460.
26. Tudor, David W.; Lewis, Terence; Robins, David J. "Synthesis of the Trifluoroacetate Salt of Aspartic Acid  $\beta$ -Semialdehyde, and Intermediate in the Biosynthesis of L-Lysine, L-Threonine, and L-Methionine." *Synthesis*. **1993**, 1061-1062.

## APPENDIX

### Appendix A: NMR Spectroscopy Data

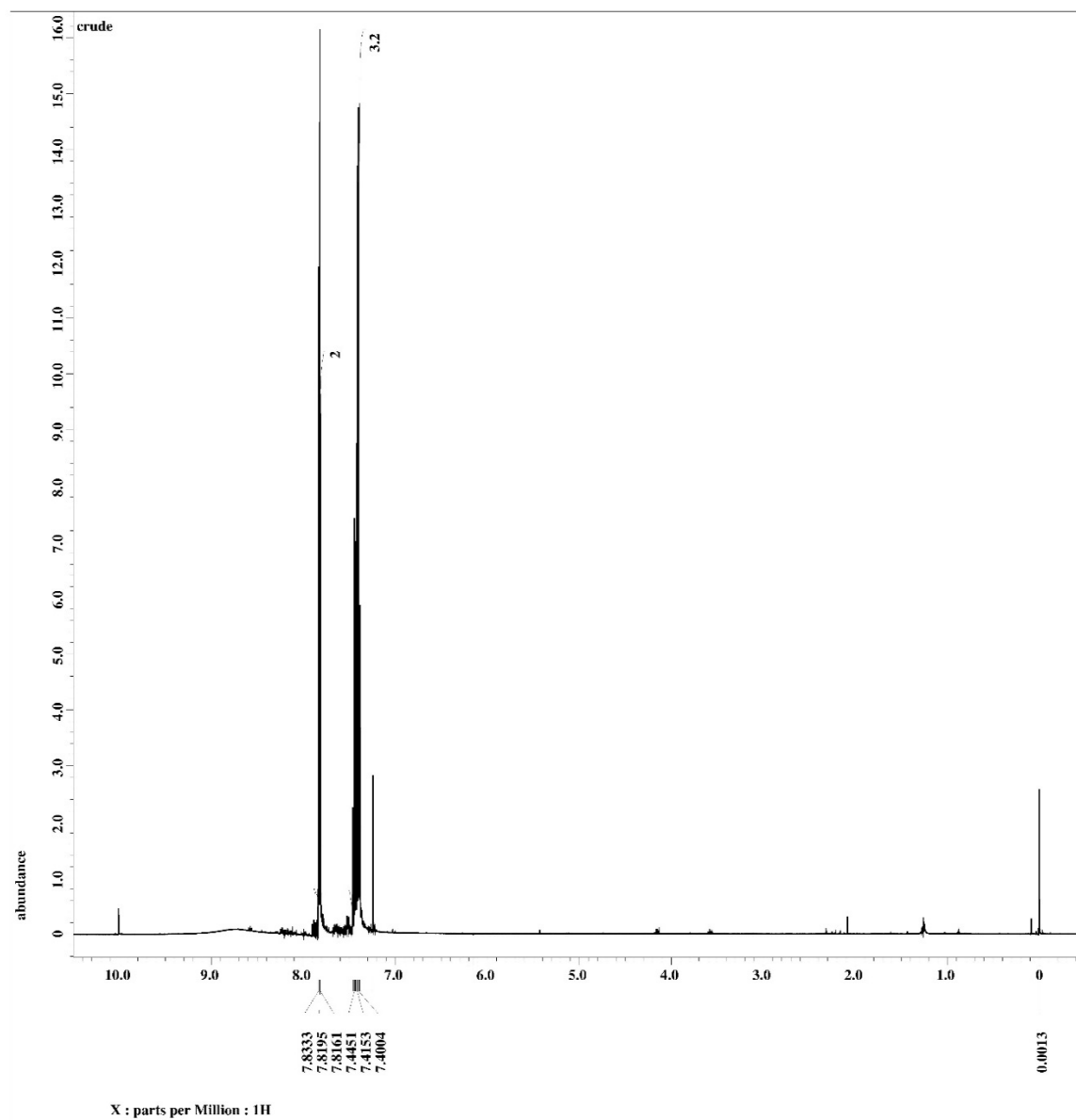
#### 1. (*E*)-Benzaldehyde Oxime

$^1\text{H}$  NMR ( $\text{CDCl}_3$ )

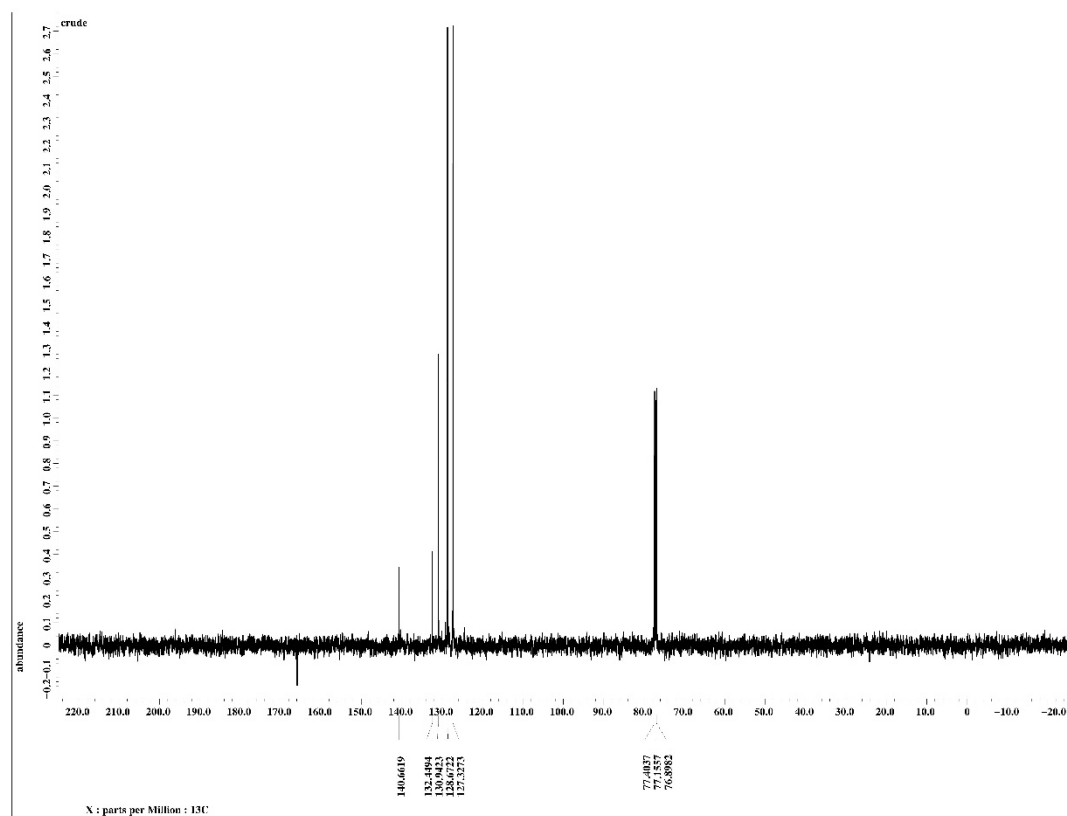


## 2. (Z)-N-Hydroxybenzimidoyl Chloride

$^1\text{H}$  NMR ( $\text{CDCl}_3$ )

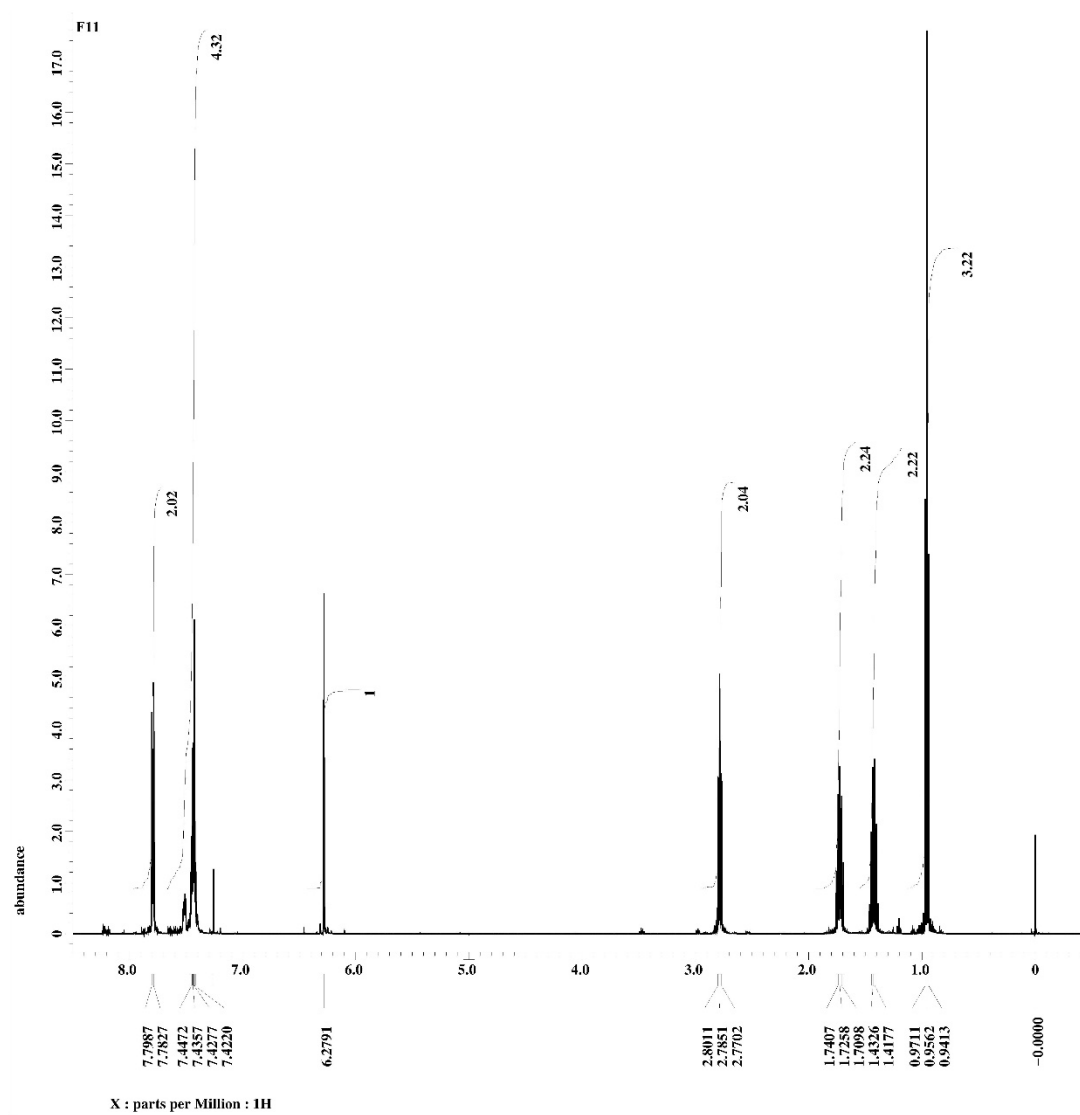


$^{13}\text{C}$  NMR ( $\text{CDCl}_3$ )

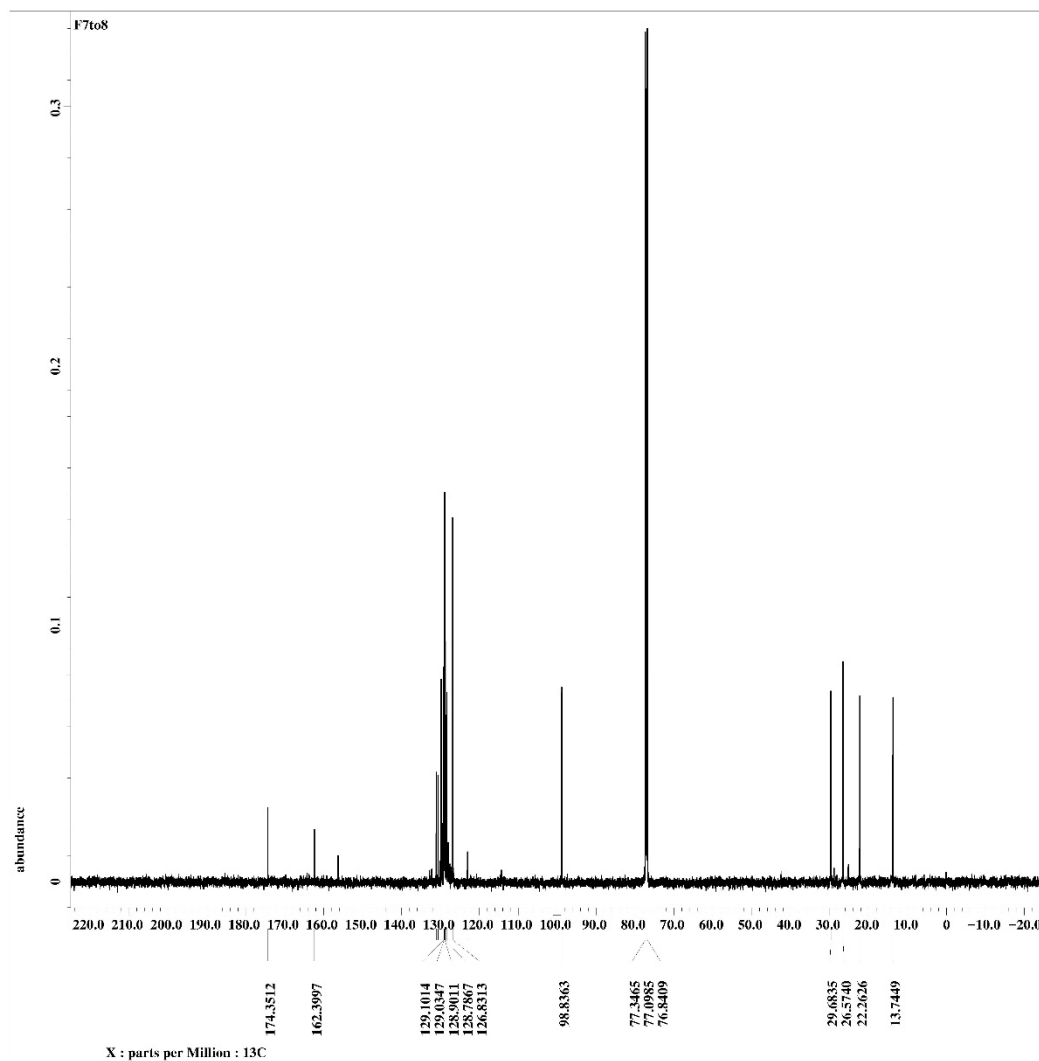


### 3. 5-Butyl-3-Phenylisoxazole

$^1\text{H}$  NMR ( $\text{CDCl}_3$ )

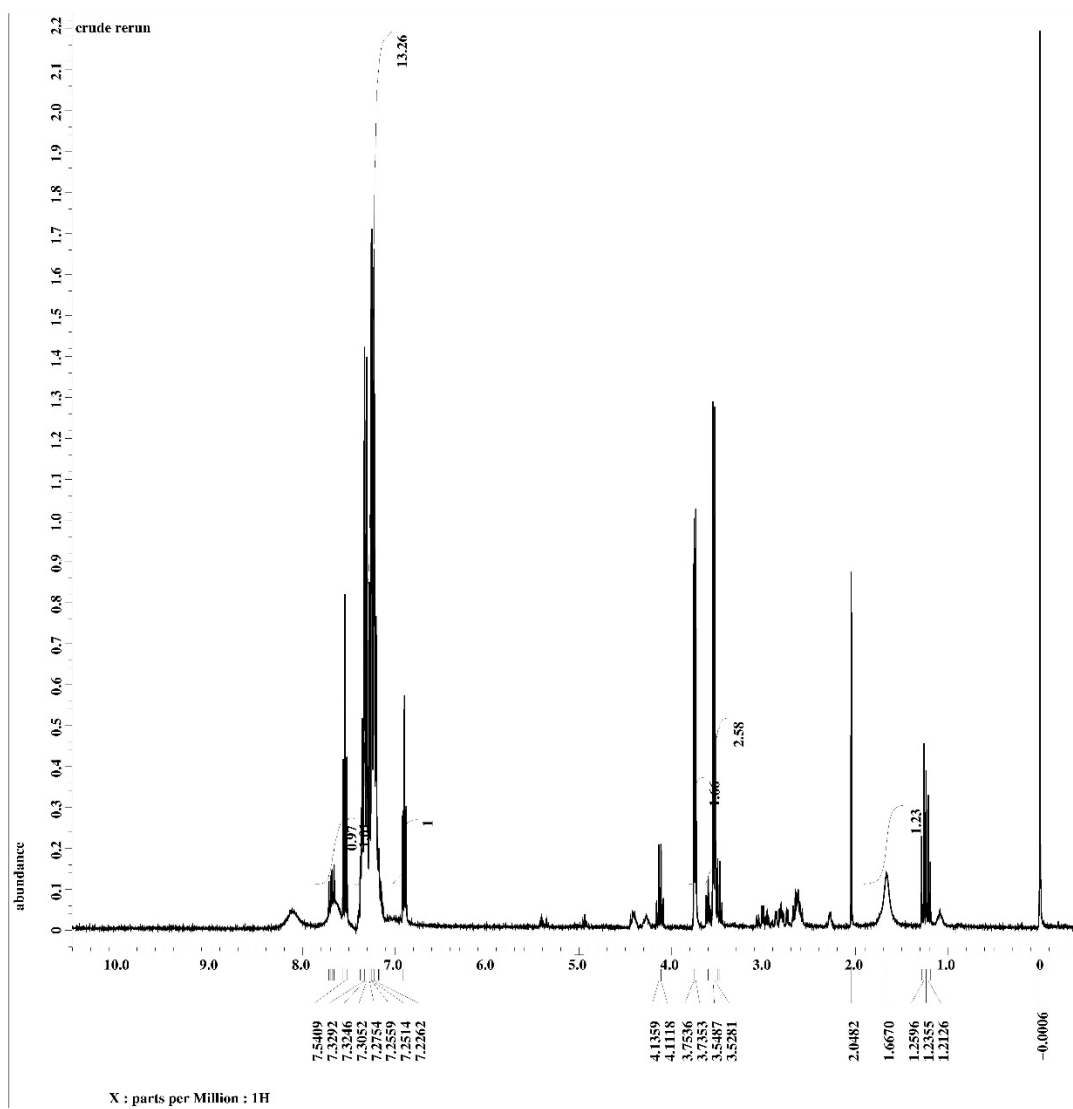


$^{13}\text{C}$  NMR ( $\text{CDCl}_3$ )



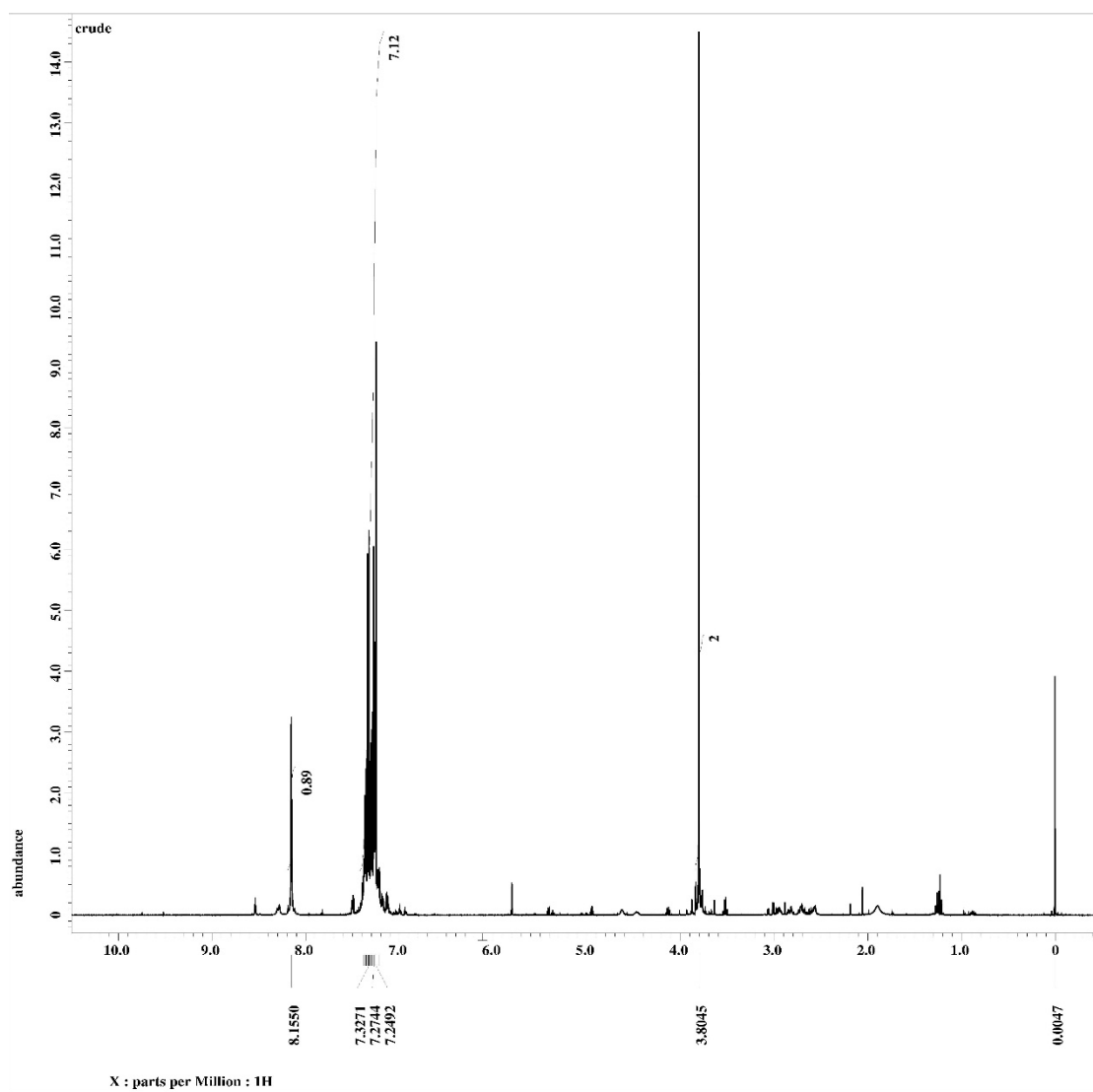
#### 4. (*E*)-2-Phenylacetaldehyde Oxime

$^1\text{H}$  NMR ( $\text{CDCl}_3$ )

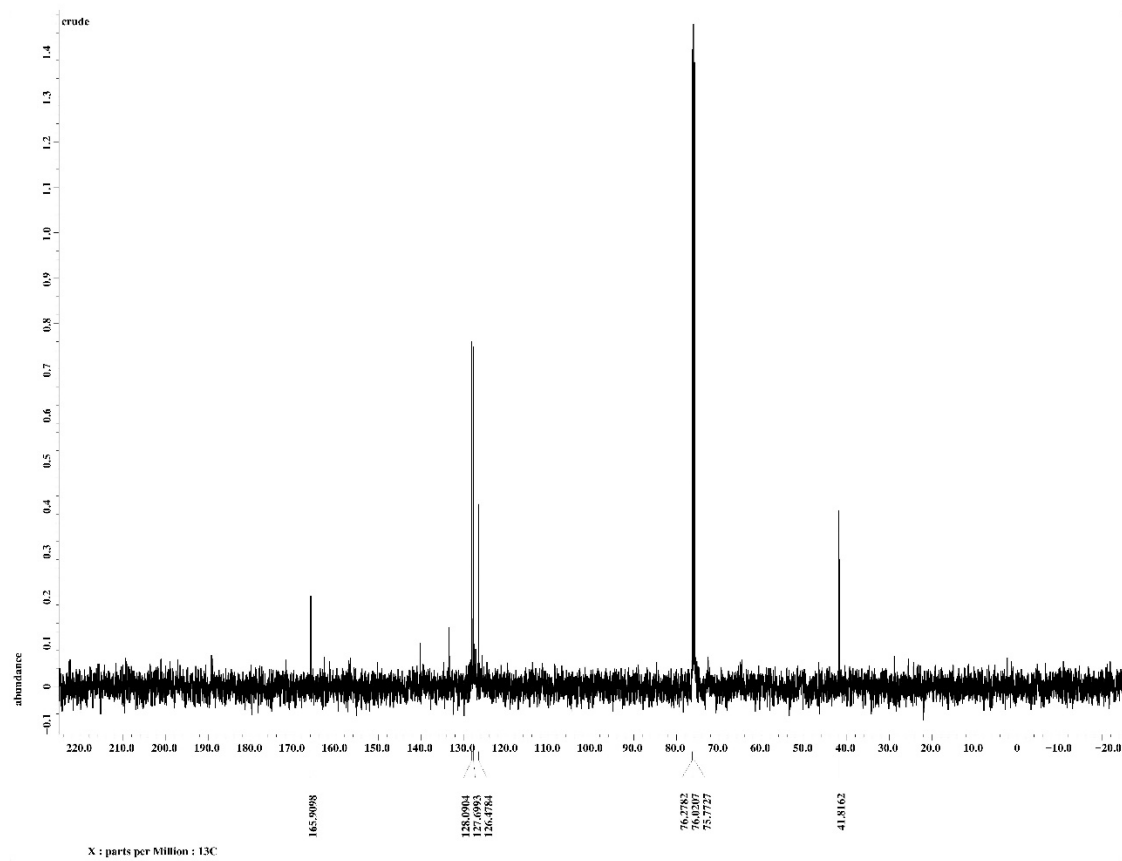


## 5. (Z)-N-Hydroxy-2-Phenylacetimidoyl Chloride

$^1\text{H}$  NMR ( $\text{CDCl}_3$ )

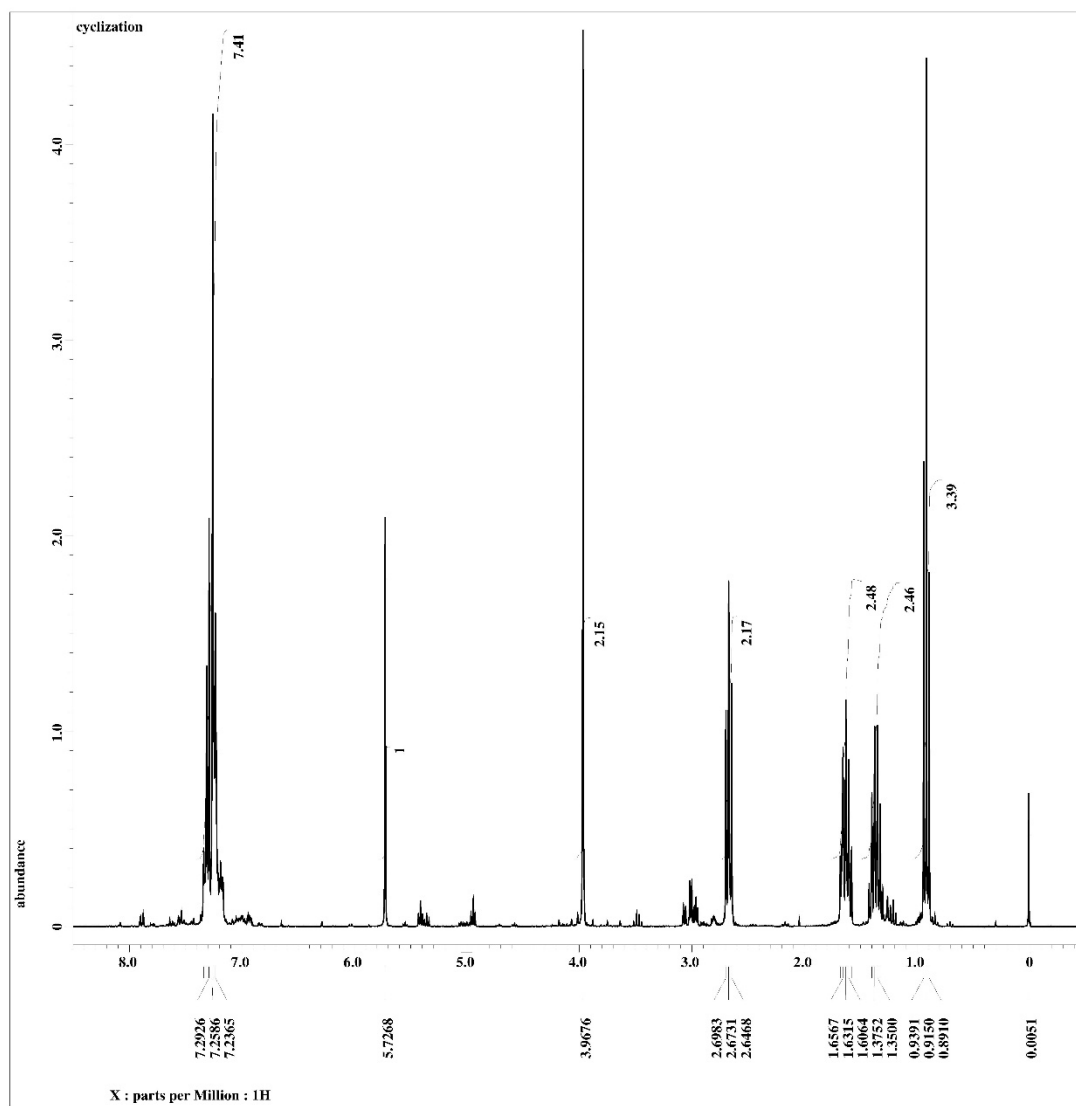


$^{13}\text{C}$  NMR ( $\text{CDCl}_3$ )

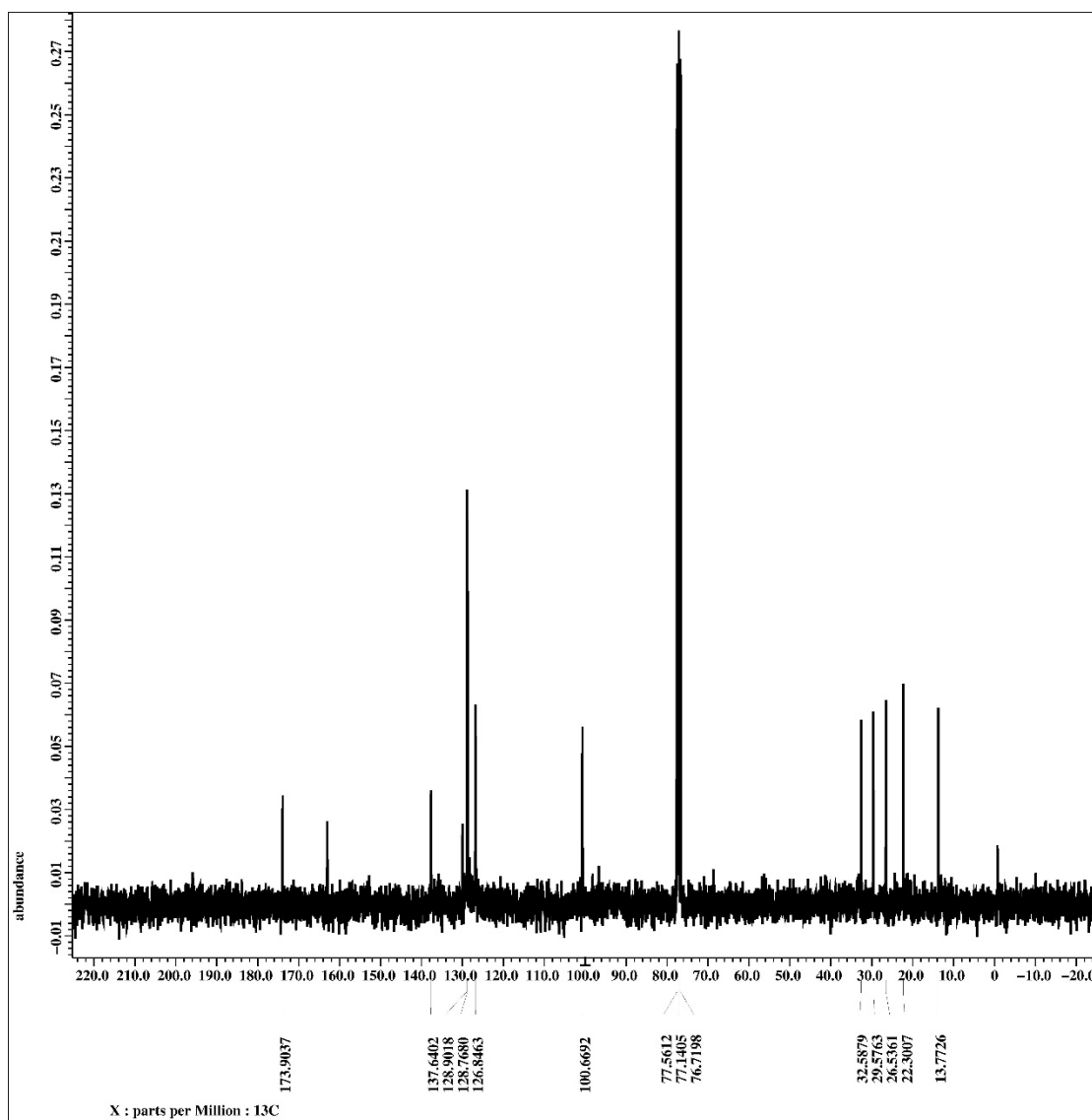


### 6. 3-Benzyl-5-butylisoxazole

$^1\text{H}$  NMR ( $\text{CDCl}_3$ )

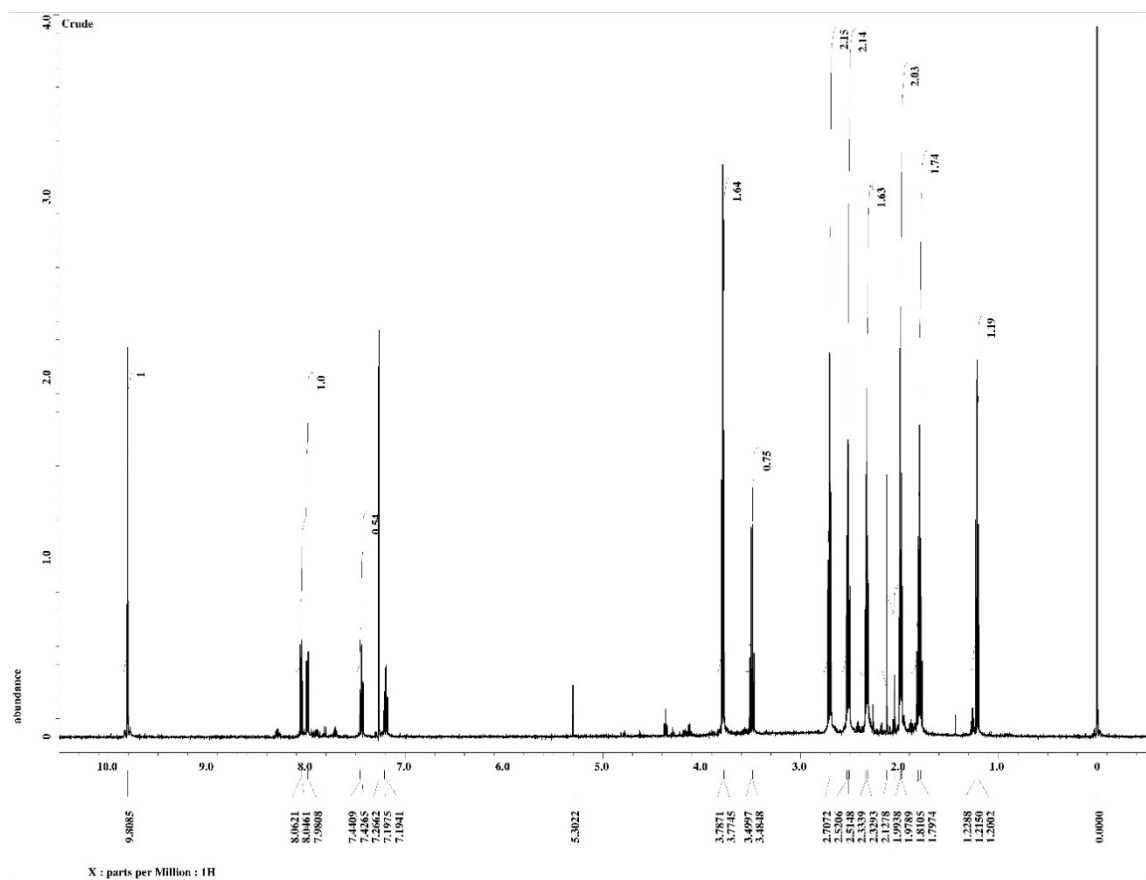


$^{13}\text{C}$  NMR ( $\text{CDCl}_3$ )



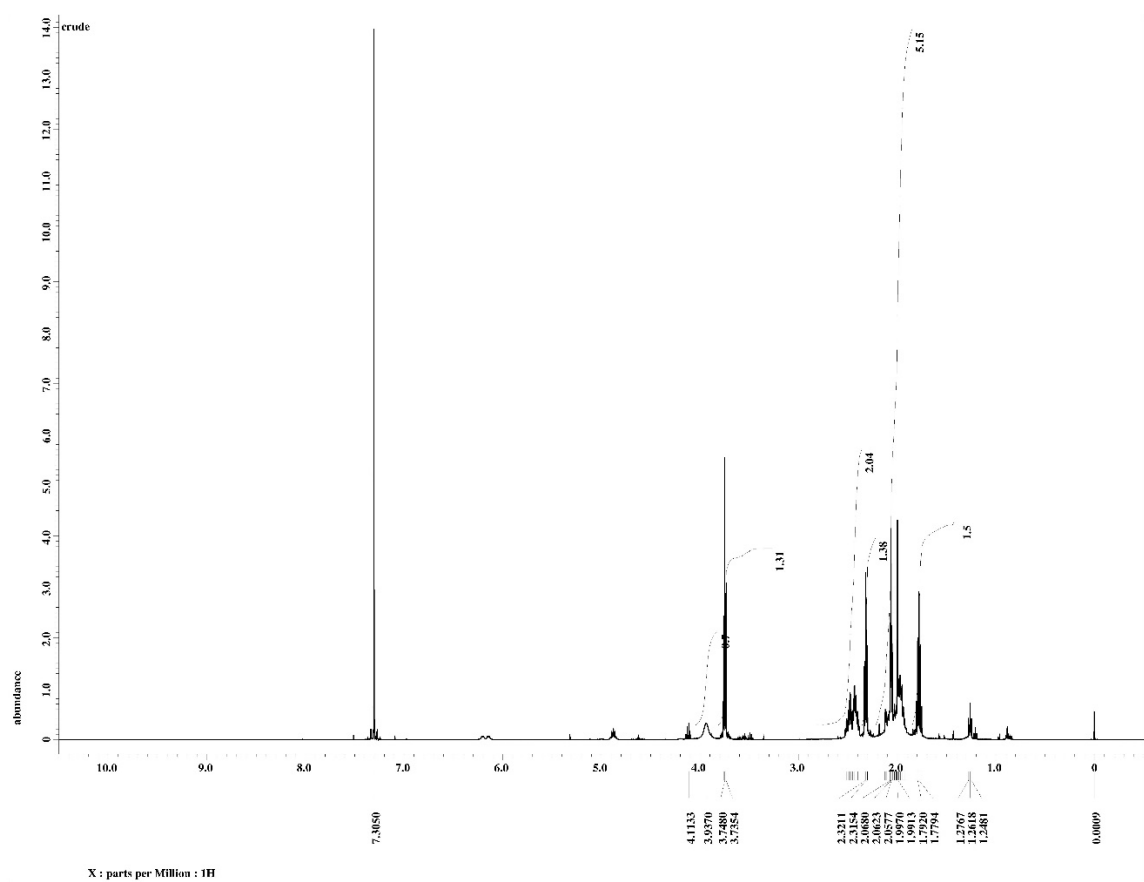
## 7. 4-Pentyn-1-al

$^1\text{H}$  NMR ( $\text{CDCl}_3$ )

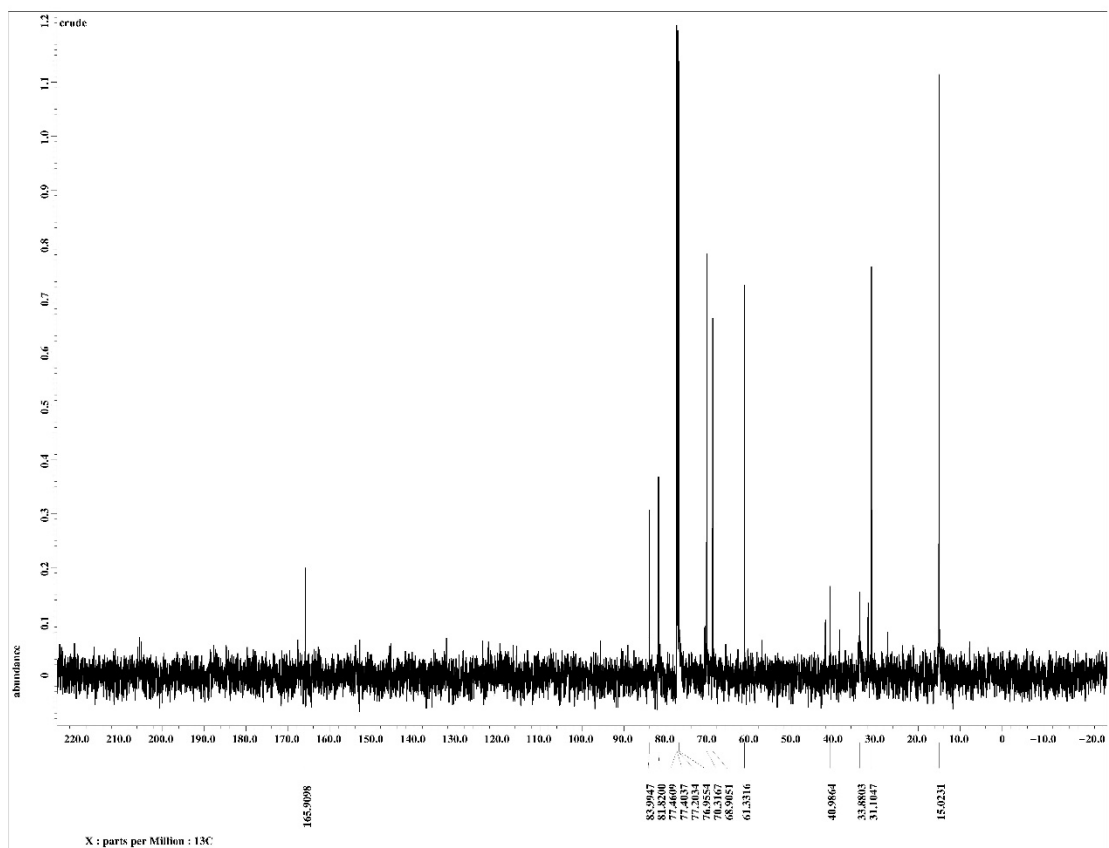


## 8. 2-Aminohept-5-ynamide

$^1\text{H}$  NMR ( $\text{CDCl}_3$ )

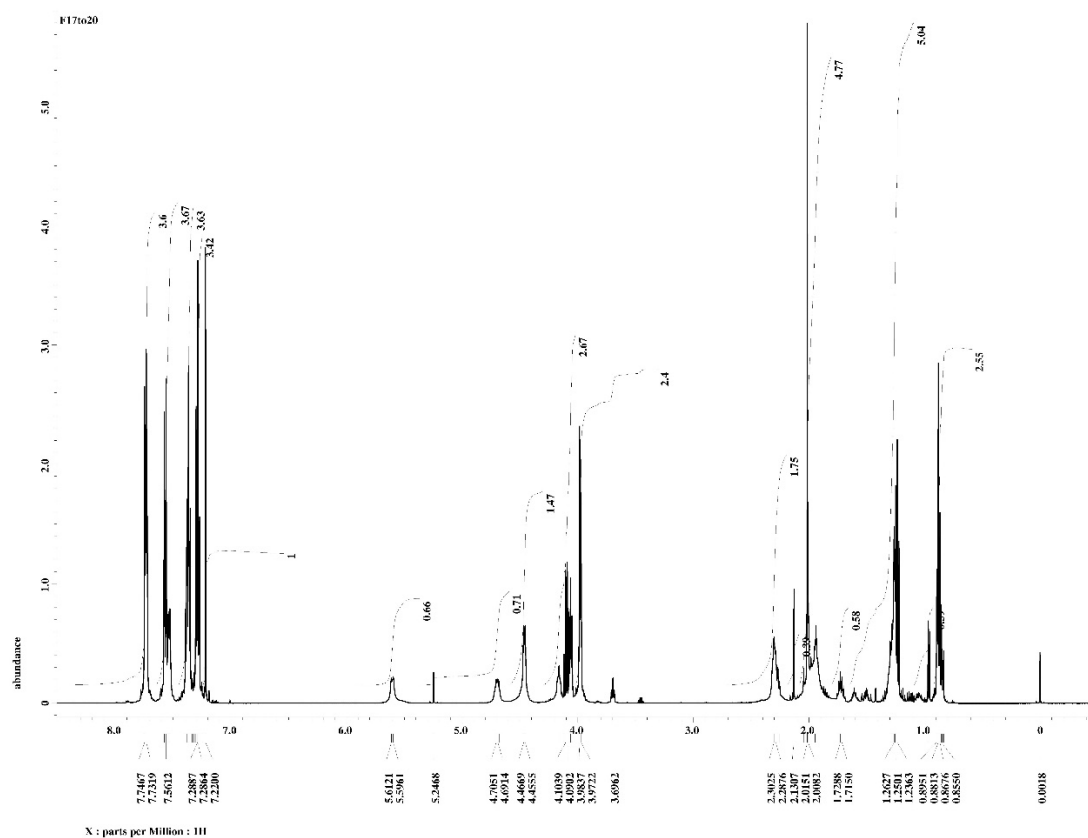


$^{13}\text{C}$  NMR ( $\text{CDCl}_3$ )

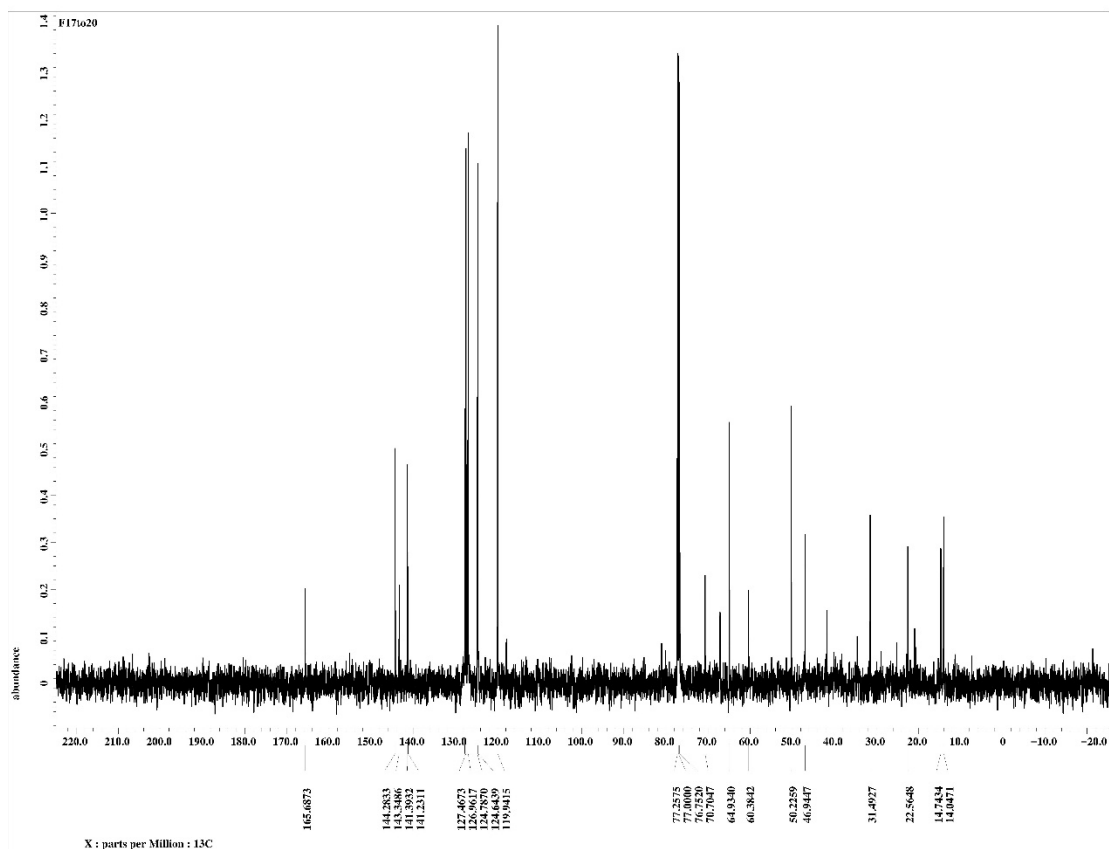


# 9. 9H-fluoren-9-yl (1-amino-1-oxohex-5-yn-2-yl) carbamate

<sup>1</sup>H NMR (CDCl<sub>3</sub>)

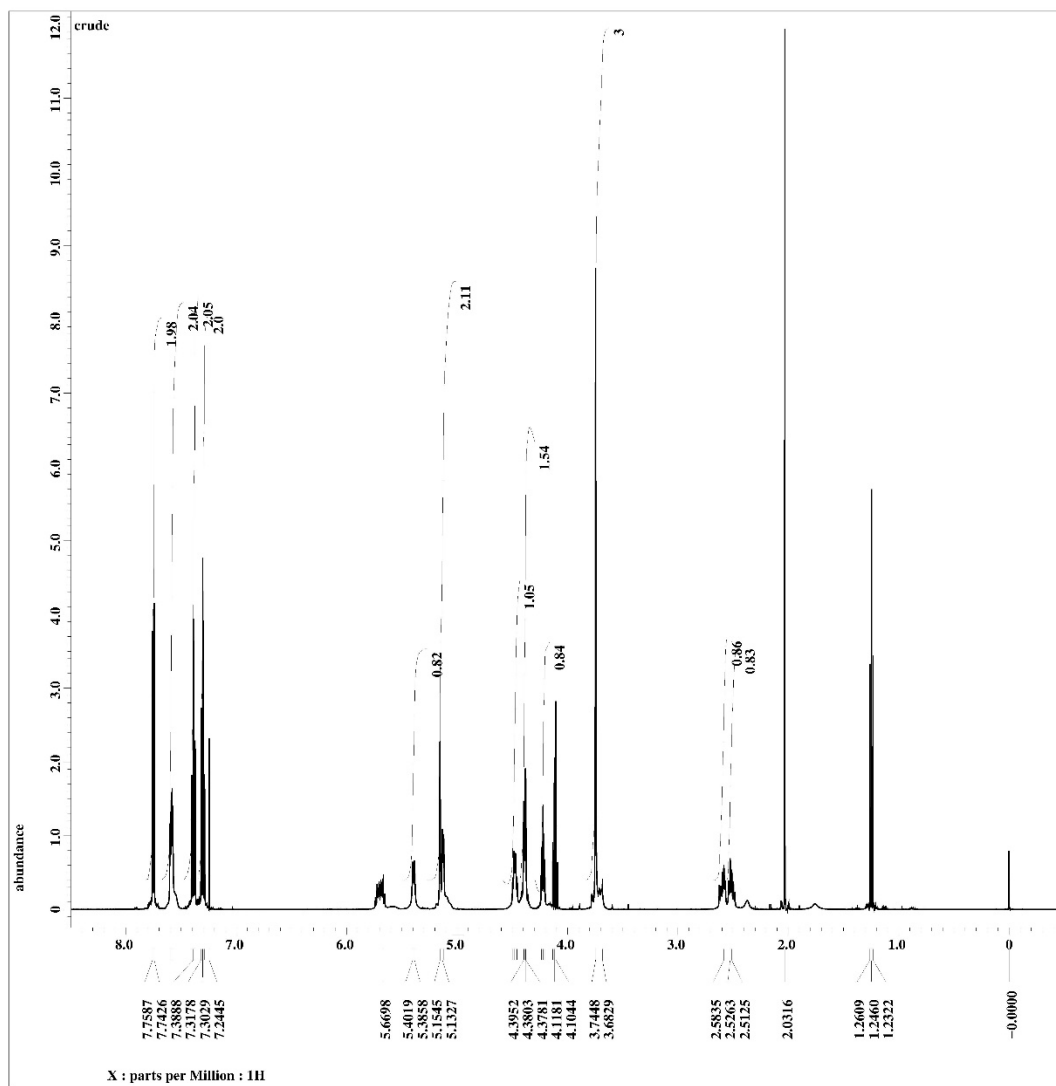


$^{13}\text{C}$  NMR ( $\text{CDCl}_3$ )

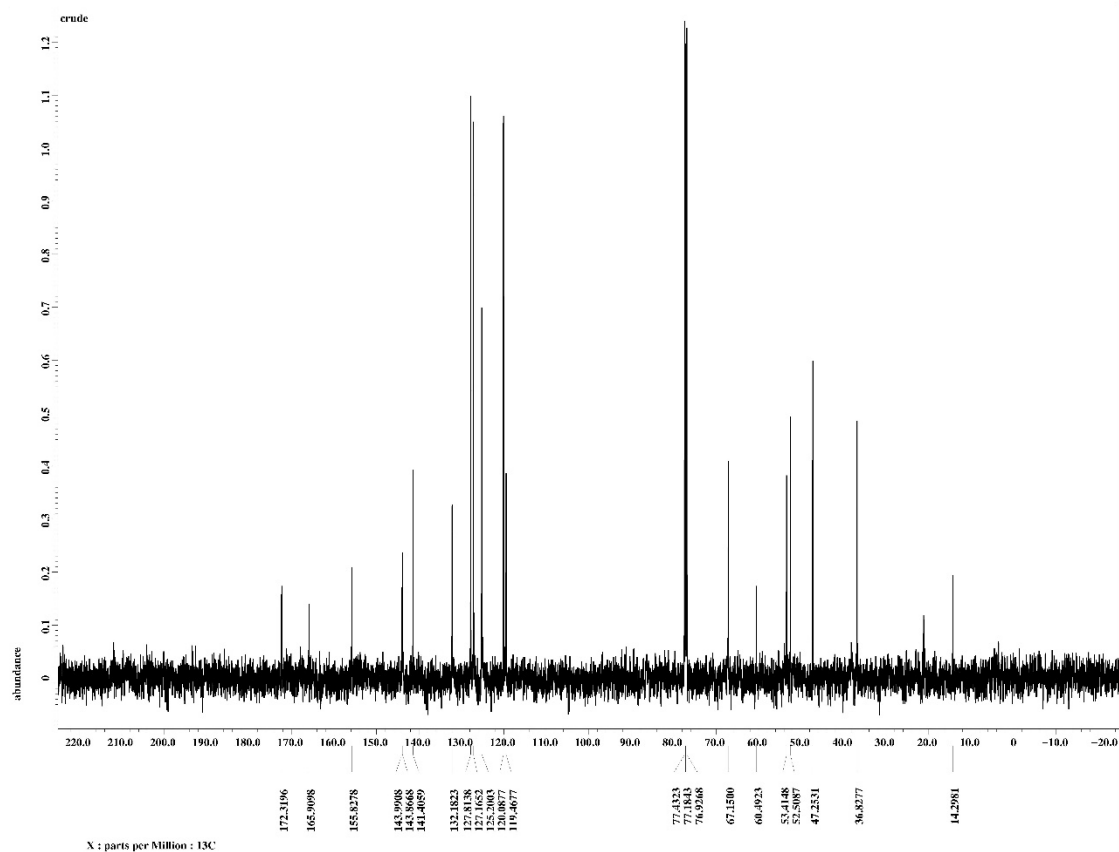


## 10. Fmoc-L-Allylglycine $\alpha$ -Methyl Ester

$^1\text{H}$  NMR ( $\text{CDCl}_3$ )

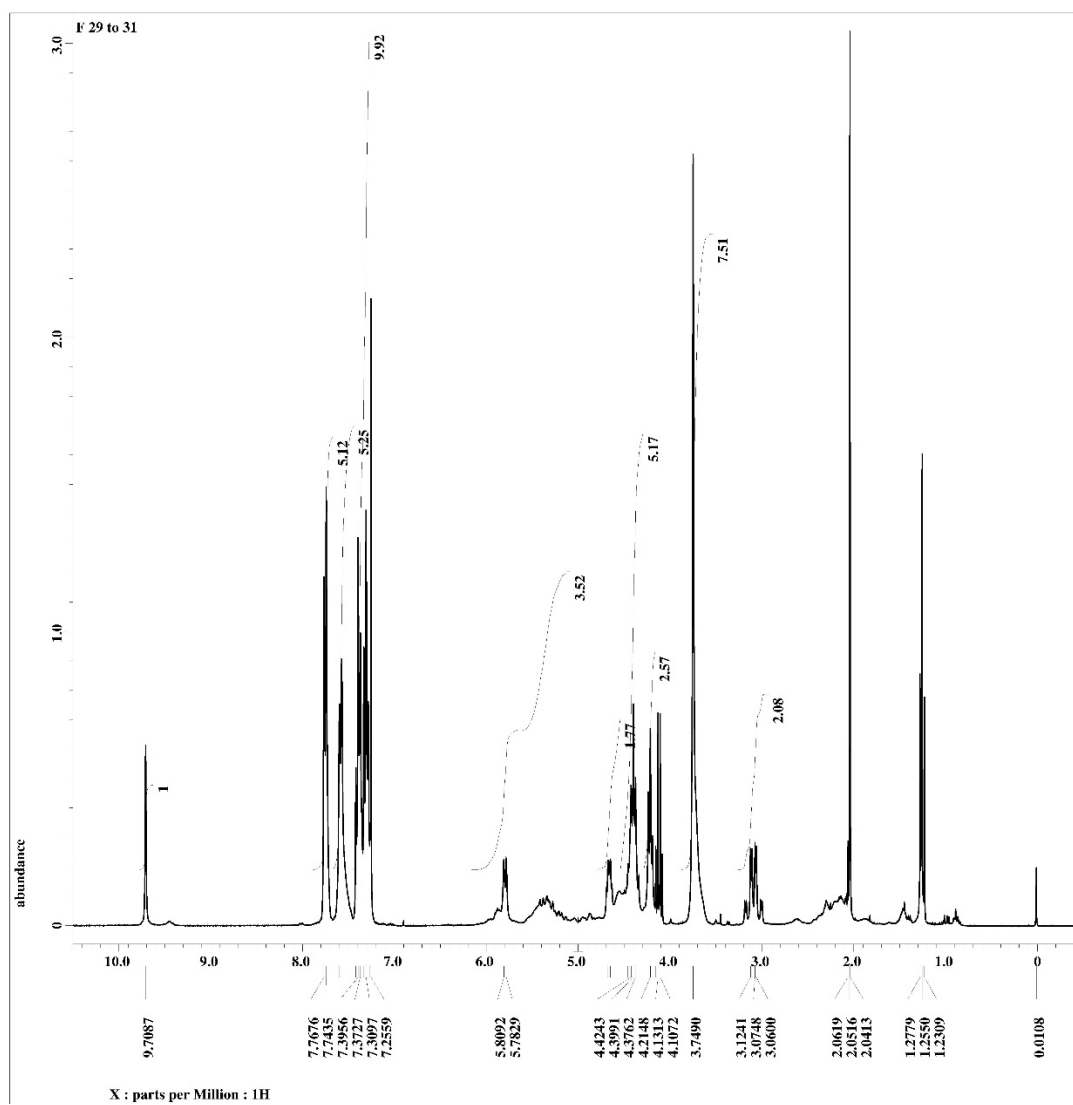


$^{13}\text{C}$  NMR ( $\text{CDCl}_3$ )



# 11. Fmoc-L-Aspartic Acid $\beta$ -Semialdehyde $\alpha$ -Methyl Ester

$^1\text{H}$  NMR ( $\text{CDCl}_3$ )



$^{13}\text{C}$  NMR ( $\text{CDCl}_3$ )

